

## Slow fission of highly excited plutonium nuclei

A. K. Sikdar,<sup>1</sup> A. Ray,<sup>1,\*</sup> Deepak Pandit,<sup>1</sup> B. Dey,<sup>1</sup> Sarmishtha Bhattacharyya,<sup>1</sup> Soumik Bhattacharya,<sup>1</sup> A. Bisoi,<sup>2,†</sup> A. De,<sup>3</sup> S. Paul,<sup>3</sup> Srijit Bhattacharya,<sup>4</sup> and A. Chatterjee<sup>5</sup>

<sup>1</sup>Variable Energy Cyclotron Centre, 1/AF Bidhannagar, Kolkata 700064, India

<sup>2</sup>Saha Institute of Nuclear Physics, 1/AF, Bidhannagar, Kolkata 700064, India

<sup>3</sup>Raniganj Girls' College, Raniganj 713358, West Bengal, India

<sup>4</sup>Department of Physics, Barasat Govt. College, Kolkata 700124, India

<sup>5</sup>Inter-University Accelerator Center, New Delhi 110067, India



(Received 18 February 2017; revised manuscript received 5 February 2018; published 14 August 2018)

**Background:** Earlier measurements of fission lifetimes of the highly excited uraniumlike nuclei by  $K$  x-ray fluorescence and crystal blocking techniques obtained slow fission (fission time  $\sim 10^{-18}$  s) for most of the fission events and were shown to be incompatible with the very short fission time ( $\sim 10^{-20}$  s) obtained by the nuclear techniques and also with the very small ( $\leq 5\%$ ) percentage of such slow fission events predicted by simple statistical models. One weakness of the earlier fluorescence experiments is that the observed  $K$  x-ray peaks were very broad [full width at half maximum (FWHM)  $\approx 15$  keV] and the precise energies of the relevant  $K$  x-ray lines could not be determined from such measurements.

**Purpose:** The purpose is to look at the relevant  $K$  x-ray energy region in coincidence with the fission fragments with a high resolution ( $\approx 1$  keV) spectrometer to obtain evidence of slow fission and determine its percentage.

**Method:** Highly excited plutonium nuclei were produced in the fusion of  ${}^4\text{He} + {}^{238}\text{U}$  at  $E({}^4\text{He})_{\text{Lab}} = 60$  MeV. The intrinsic width of plutonium  $K$  x-ray lines in coincidence with the fission fragments was determined as a direct measure (or lower limit) of the fission time of the slow ( $\sim 10^{-18}$  s) fission events. The minimum percentage of slow fission events has been determined from the  $K$  x-ray multiplicity per fission event and the probability of creation of  $K$ -orbital vacancies in plutonium.

**Results:** A narrow peak (FWHM  $\approx 1$  keV) observed in the coincidence photon spectrum at  $(102.8 \pm 0.5)$  keV, just below the characteristic plutonium  $K_{\alpha 1}$  line (103.7 keV) has been attributed to the plutonium  $K_{\alpha 1}$  line on the basis of supporting evidence and calculations and we deduce that most of the fission events are slow (fission time  $> 10^{-18}$  s). No peak has been observed exactly at 103.7 keV.

**Conclusions:** The shift  $[(0.9 \pm 0.5)$  keV] of plutonium  $K$  x-ray lines is plausible, if the fissioning plutonium nucleus spends most of its long fission time in a highly deformed dumbbell shape (beyond saddle) and the corresponding results are in agreement with those obtained earlier by the atomic techniques. Alternatively, if no significant shift of plutonium  $K$  x-ray lines can be expected, the absence of a peak at 103.7 keV contradicts earlier atomic technique claims of a significant percentage of slow fission events.

DOI: [10.1103/PhysRevC.98.024615](https://doi.org/10.1103/PhysRevC.98.024615)

### I. INTRODUCTION

Nuclear fission is one of the most important discoveries of the 20th century and in this context, the fission dynamics of highly excited fissile nuclei has a special significance. The time scale of the nuclear fission process of highly excited fissile nuclei is a basic characteristic of the underlying fission dynamics. However, atomic techniques ( $K$  x-ray-fission fragment coincidence and crystal blocking techniques) [1–6] have deduced long fission times ( $\sim 10^{-18}$  s) for most of the fission events of highly excited fissile nuclei, whereas nuclear techniques and calculations [7–11] have obtained much

shorter fission time ( $\sim 10^{-20}$  s). Both the nuclear and atomic techniques are sensitive to the time that elapses between the formation of the fissioning nucleus to its scission. This time is generally called the fission time. Hereinafter, we distinguish two fission lifetime ranges: fission lifetimes  $> 10^{-18}$  s will be referred to as long fission time or slow fission events and fission lifetimes  $< 10^{-19}$  s will be referred to as short fission time. Bulgac *et al.* [11] performed fission dynamics calculations using a density functional technique and obtained short saddle to scission times for excited ( $E_X = 8$  MeV)  ${}^{240}\text{Pu}$  nuclei. A distribution of fission times stretching to very long fission time scales has been obtained from Langevin fluctuation-dissipation dynamical calculations [12,13] and the percentage of fission events having long fission times could be increased arbitrarily by increasing the viscosity parameter. The vastly different fission time scales as deduced from the nuclear and atomic techniques have been attributed to the sensitivity of the techniques to different time domains [12,13]. It was argued

\*Corresponding authors: ray@vecc.gov.in; amlanray2016@gmail.com

†Present Address: Department of Physics, Indian Institute of Engineering Science and Technology, Shibpur, Howrah 711103, India.

that the observed long fission times could provide information about the viscosity [12,13] of the nuclear medium and might be used as a probe [4] for studying the production of long-lived superheavy nuclei. It was recently shown [14] that the observed long fission time for the majority of the fissioning events as obtained by the atomic techniques cannot be reconciled with the short fission time obtained by the nuclear techniques for any plausible fission time distribution. So, it is very important to examine the evidence for long fission time in more detail.

In earlier  $K$  x-ray fluorescence experiments [1,6], fissioning compound nuclei were produced in high energy heavy ion fusion and deep-inelastic reactions. In these reactions, a number of elements with similar  $Z$  values was produced and the closely spaced, unresolved  $K$  x-ray lines from these elements produced very broad [full width at half maximum (FWHM)  $\approx 15$ – $20$  keV]  $K$  x-ray bumps. In addition, the electronic configuration mixing significantly broadened  $K$  x-ray lines [6]. So, it was not possible to know the precise energies of the relevant  $K$  x-ray peaks from such measurements.

The intrinsic width of the relevant  $K$  x-ray lines is expected to increase in inverse proportion to the fission time, in accordance with the quantum energy-time uncertainty principle, thus providing a direct measure of the fission time [15]. In earlier experiments [1,6], both the minimum time and percentage of slow fission events were deduced from the measured  $K$  x-ray multiplicity per fission, known atomic  $K$ -vacancy lifetime, and the estimated probability of creation of  $K$  orbital vacancies ( $P_K$ ) in the element produced by the fusion or deep inelastic collision process.

In order to obtain more detailed evidence regarding the presence of a significant percentage of slow fission events, it is important to look at the relevant  $K$  x-ray regions with a high energy resolution ( $\approx 1$  keV) to identify the relevant peaks. Since heavy ion reactions would result in broadening of the  $K$  x-ray peak from the composite element, we bombarded a natural uranium target with a 60-MeV  ${}^4\text{He}^{2+}$  beam and produced  ${}^{242}\text{Pu}$  nucleus at  $E_X \approx 55$  MeV. In this reaction, plutonium produced by fusion would primarily be the element undergoing fission without the complication of incomplete fusion. Electronic configuration mixing is also expected to be small for  ${}^4\text{He} + {}^{238}\text{U}$  fusion reaction. Hence, for  ${}^4\text{He} + {}^{238}\text{U}$  reaction, we expect to see narrow plutonium  $K$  x-ray lines in coincidence with the fission fragments if a significant percentage of long-lived fission time component is present. The fission time of slow fission events could then be determined from the increase of the intrinsic width of the  $K$  x-ray lines using the quantum energy-time uncertainty principle in a completely model independent way. Unlike the method used in Refs. [5,6], the determination of fission time from the intrinsic width of  $K$  x-ray line does not require any knowledge of any other parameters such as  $P_K$  that is always difficult to determine precisely in a fusion reaction. However, the minimum percentage of slow fission events cannot be determined from the width of the  $K$  x-ray peak and has to be determined in the usual way [5,6] from the measured  $K$  x-ray multiplicity per fission event and value of  $P_K$ . Narrow characteristic  $K$  x-ray lines from the atom/ion [16,17] were seen before by inelastic scattering of low energy protons ( $E_{\text{Lab}} = 10$ – $12$  MeV) from  ${}^{112}\text{Sn}$  and  ${}^{106}\text{Cd}$  targets and from evaporation residues [18,19] in heavy ion induced

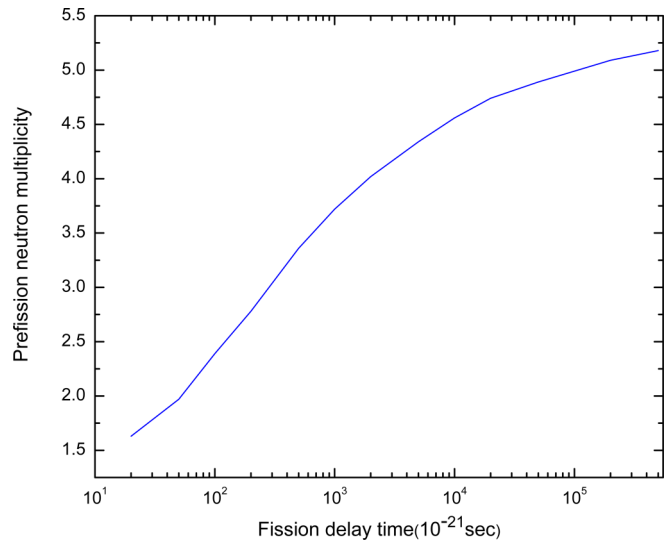


FIG. 1. Fission delay time vs pre-fission neutron multiplicity for  ${}^4\text{He} + {}^{238}\text{U}$  reaction at  $E_{\text{LAB}}({}^4\text{He}) = 60$  MeV as obtained from JOANNE2 code calculations.

reaction. However, such narrow  $K$  x-ray peaks have not been seen so far from an atom/ion containing a fissioning nucleus, because the probability of creation of  $K$ -orbital vacancy ( $P_K$ ) in a uraniumlike heavy element is very small by proton or alpha projectile compared to a high  $Z$  projectile, thus making such measurements rather challenging.

Simple statistical model codes [20,21] that do not consider possible dynamical effects as arising from viscosity in the passage from saddle to scission predict a very small percentage ( $\leq 5\%$ ) of slow fission events for  ${}^4\text{He} + {}^{238}\text{U}$  reaction at  $E_{\text{LAB}}({}^4\text{He}) = 60$  MeV, because a relatively large number of competing neutrons would be emitted prior to such a slow fission event, thus significantly reducing the excitation energy of the fissioning nucleus and the corresponding fission cross section. In Fig. 1, we show a plot of fission delay time versus prefission neutron multiplicity for  ${}^4\text{He} + {}^{238}\text{U}$  reaction at  $E_{\text{LAB}}({}^4\text{He}) = 60$  MeV as obtained from the JOANNE2 code [20]. It is seen from Fig. 1 that the prefission neutron multiplicity is predicted to be  $>4$  for fission delay time  $>10^{-18}$  s. Measured prefission neutron multiplicities [10] in this mass and excitation energy range are  $\approx 2$ , indicating an average fission delay time on the order of  $10^{-20}$  s and the contribution of slow fission events is expected to be  $<5\%$ .

It is possible to significantly increase the calculated contribution of the long-lived fission component by considering large values of the viscosity parameter in the framework of the Langevin fluctuation-dissipation dynamical model [12,13]. The  $K$  x-ray technique is sensitive to such long-lived fission events. The goal of our  $K$  x-ray-fission fragment coincidence experiment is to look at the relevant  $K$  x-ray region in the coincidence photon spectrum with a high energy resolution of  $\approx 1$  keV to explore evidence for the presence of significant percentage of slow fission events. It should be noted that the determination of the fission time by the  $K$  x-ray technique is significantly biased towards the long fission time component, because the fission events with a short fission time would

produce a very broad and weak  $K$  x-ray peak that would not be observable above the fission fragment  $\gamma$ -ray background.

## II. EXPERIMENTAL PROCEDURE

A natural uranium-oxide film ( $\approx 2.5$  mg/cm<sup>2</sup> thick) electrodeposited on a thin aluminum foil (thickness  $\approx 1$  micron) was bombarded by a beam of 60 MeV  $^4\text{He}$  particles ( $\approx 2$  pA beam current) accelerated by the Variable Energy Cyclotron located in Kolkata, India. The photovoltaic cell can be used as a fission fragment detector even in the presence of an intense background of lightly ionizing particles such as protons and alpha particles [22], because the pulses produced by the fission fragments in a photovoltaic cell are much larger than those produced by the lightly ionizing particles. Two such photovoltaic cells of dimensions 2.5 cm  $\times$  1.25 cm were mounted on a printed circuit board and electrically connected to give a single output. The photovoltaic cell detector assembly was placed at a distance of  $\approx 2$  cm from the target to detect fission fragments and it covered about 10% of the  $4\pi$  solid angle. The center of the photovoltaic cell detector assembly was at  $135^\circ$  with the beam axis and covered an angular range of  $120$ – $150^\circ$  in the horizontal plane. Energy calibration of the photovoltaic cell detector assembly was done by using a  $^{252}\text{Cf}$  fission fragment source.

A four-segmented high purity planar germanium low energy photon spectrometer (LEPS) with an active area of  $4 \times 80$  mm<sup>2</sup> was placed at a distance of 10.7 cm from the target at a polar angle of  $90^\circ$  to the beam direction. Each segment of LEPS subtended a solid angle of about 7 milliradians (msr) and detected low energy  $\gamma$  rays and x rays. There was a thin beryllium window (thickness = 0.127 mm) to maintain high vacuum inside the detector for keeping crystal purity. The experiment was performed in an aluminum scattering chamber with a wall thickness of about 2 mm.  $\gamma$  rays and x rays produced in the reaction passed through the thin wall of the scattering chamber and beryllium window to reach the LEPS and so the 20-keV uranium  $L$  x rays reaching the detector were strongly attenuated. The energy spectra of the four crystals were calibrated individually using  $^{133}\text{Ba}$ ,  $^{152}\text{Eu}$ , and  $^{241}\text{Am}$   $\gamma$ -ray sources. The efficiency curve for each crystal of the LEPS was obtained by placing calibrated  $\gamma$ -ray sources at the target position. In order to obtain photon spectrum in coincidence with the fission fragments from  $^4\text{He} + ^{238}\text{U}$  reaction, a coincidence between the photovoltaic cell detector assembly and LEPS was required and data were taken whenever any crystal of the LEPS recorded a  $\gamma$ -ray or x-ray event. The large capacitance and high count rate of the large photovoltaic cell detector assembly made it necessary to work with slow energy signals (having long rise time) from the preamplifier resulting in relatively large coincidence window of  $2.5 \mu\text{s}$ .

## III. DATA ANALYSIS AND EXPERIMENTAL RESULTS

Fission fragment spectra recorded by the photovoltaic cell detector assembly in coincidence with the x rays and  $\gamma$  rays detected by the LEPS were obtained for each run by gating on a  $2.5$ - $\mu\text{s}$  coincidence time window. Random coincidences were subtracted by appropriately gating on both sides of

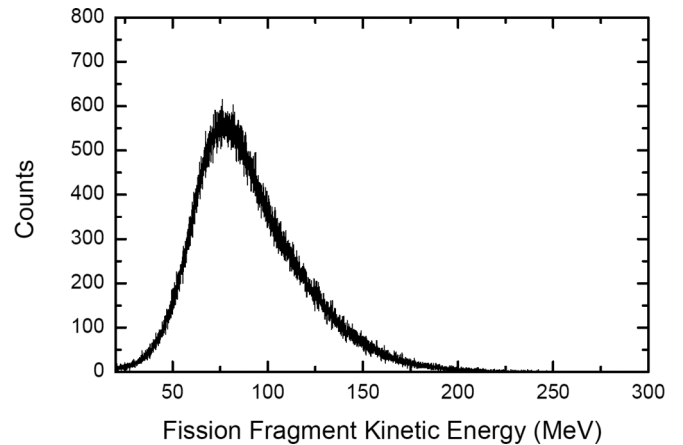


FIG. 2. Fission fragment spectrum in coincidence with the LEPS detector for  $^4\text{He} + ^{238}\text{U}$  reaction at  $E_{\text{LAB}}(^4\text{He}) = 60$  MeV.

the prompt peak in the time spectrum. The fission fragment spectra looked clean and had the expected shape. A typical fission fragment spectrum (in coincidence with LEPS) from a run is shown in Fig. 2. The thick uranium oxide target resulted in a shift of the peak position of the fission fragment spectrum towards the lower energy and a tailing on the high energy side. The energy calibrated photon spectra of the LEPS crystals were added for all the runs to obtain the final photon spectrum. In Fig. 3 (top panel), we show the final prompt photon spectrum (in the energy region from 45 to 120 keV) obtained by gating on a  $2.5$ - $\mu\text{s}$  coincidence time window. The red curve (upper panel of Fig. 3) shows the background. In the lower panel of Fig. 3, we show the background subtracted

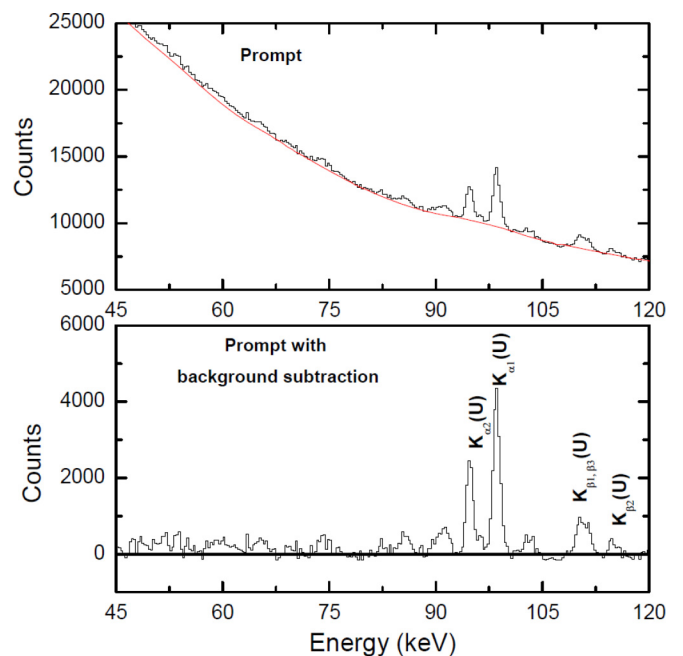


FIG. 3. Prompt gated photon spectrum with a red background (upper panel). Prompt gated and background subtracted photon spectrum (bottom panel).

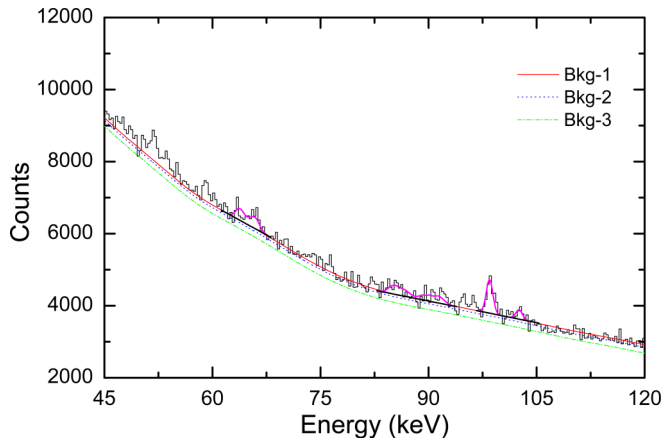


FIG. 4. Random coincidence corrected photon spectrum and different backgrounds shown by Bkg-1 (solid red), Bkg-2 (dotted blue), and Bkg-3 (dot-dashed green) curves. Different peaks are shown in magenta color (see text for details).

prompt spectrum where strong uranium  $K_{\alpha 1}$  (98.4 keV),  $K_{\alpha 2}$  (94.6 keV),  $K_{\beta 1}$  (111.3 keV),  $K_{\beta 2}$  (114.4 keV), and  $K_{\beta 3}$  lines (110.4 keV) arising from the excitation of the uranium atom by the  $^4\text{He}$  particles are seen. A broad bump is seen around 103 keV. Since the cyclotron beam bursts were 10 ns wide and separated by about 110 ns, the prompt spectrum includes random coincidence events. The photon spectrum in random coincidence (obtained by appropriately gating on both sides of the prompt peak in the time spectrum) was subtracted out from the prompt spectrum channel by channel. The resulting photon spectrum in true coincidence with the fission fragments is shown in Fig. 4 (in the energy region from 45 to 120 keV). We see small peaks riding on a large background. Besides plutonium  $K$  x-ray lines of our interest, uranium  $K$  x-ray lines arising from inelastic scattering could be present in the coincidence spectrum due to imperfect cancellation of random coincidences. Additionally, fission fragment  $\gamma$  rays produce a large background. It is possible to differentiate between the fission fragment  $\gamma$ -ray peaks and plutonium  $K$  x-ray peaks from their spectral shapes. The fission fragment  $\gamma$ -ray line would be significantly Doppler broadened (source velocities  $\approx 0.04c$ , with  $c$  being the speed of light in vacuum) because of the large angular coverage ( $120$ – $150^\circ$ ) of the detected fission fragments. Moreover, these peaks would be double humped because of emission from the detected and complementary fragments. On the other hand,  $K$  x-ray photons from the slowly moving plutonium atom (speed  $\approx 0.003c$  along the direction of the beam axis) detected by LEPS at  $90^\circ$  would produce isolated sharp  $K$  x-ray lines for slow fission events and could be distinguished from broad, double-humped fission fragment  $\gamma$ -ray peaks. However, in the case of short fission lifetime events, the plutonium  $K$  x-ray peaks would be very broad and cut out by the background line. Another criterion to discriminate between the plutonium  $K$  x-ray lines and fission fragment  $\gamma$  rays is by gating on different parts of the fission fragment kinetic energy spectrum. Since the fission fragment kinetic energy spectrum is related to the fragment mass spectrum, fission fragment  $\gamma$  rays would come from specific regions of the fission fragment

energy spectrum, whereas all regions of the fission fragment kinetic energy spectrum would contribute to plutonium  $K$  x-ray lines. An appropriate background curve has to be drawn to carry out the analysis and determine the areas and widths of the peaks of interest. We discuss in the next sections the method used to draw the best background curve and discuss what happens as we lower the background curve.

### A. Drawing of backgrounds

In the random corrected true coincidence spectrum (Fig. 4), small peaks ride on a large background. We have performed fits with linear backgrounds and find that the data points around 103 and 98.4 keV can be best fitted by narrow Gaussian peaks with  $\text{FWHM} = 1$  keV. The magenta color curves show the best fit Gaussian peaks and the corresponding linear backgrounds are shown by black lines. The typical reduced  $\chi^2$  is  $\approx 1$  with confidence level  $\approx 99\%$  (ratio of peak area to statistical error bar  $\approx 3$ ) for the data points around 103 keV (from 100.5 to 105.3 keV) with a linear background. If, instead, a broad Gaussian peak with  $\text{FWHM} = 3$  keV is tried, the peak around 103 keV becomes poorly defined (ratio of peak area to statistical error  $\approx 1.6$ ). Hence, clearly a narrow Gaussian peak centered around 103 keV ( $\text{FWHM} = 1$  keV) is statistically the best description of the data points in the region spanning 100.5 to 105.3 keV. Broad double-humped peak structures are seen around 65 and 88 keV and they could be best fitted by GEANT3 [23] simulated curves obtained by using actual experimental geometry and linear backgrounds (black lines). In this way, we have obtained best-fitted linear backgrounds (black lines) under different narrow and broad peaks. A smooth curve (solid red curve) has been drawn by joining these black straight lines and it has been taken as the best background curve (labeled Bkg-1 in Fig. 4). In order to see the sensitivity of our results to small changes in drawing background, another curve, Bkg-2 (dotted blue curve), was drawn slightly below Bkg-1. We have also drawn a much lower background curve, Bkg-3 (dot-dashed green curve), and discussed whether such a low background is reasonable.

#### 1. Analysis with Bkg-1

The upper panel in Fig. 5 shows the data along with background curve Bkg-1 and the lower panel shows the background subtracted spectrum. We find from the background subtracted true coincidence spectrum [Fig. 5 (lower panel)] that all the uranium  $K$  x-ray lines have been suppressed by a large factor compared to their intensities in the prompt gated spectrum [Fig. 3 (lower panel)]. Although uranium  $K$  x-ray lines ideally should not at all be present in the background subtracted true coincidence spectrum, we see a relatively intense peak around 98.4 keV in the true coincidence spectrum. This peak could partly be due to the remnant of uranium  $K_{\alpha 1}$  line arising from imperfect cancellation of random coincidence events. The remnants of 94.65-keV uranium  $K_{\alpha 2}$  lines are also present. New peaks such as double-humped broad peaks at 65 and 88 keV emerged (Fig. 5) in the coincidence spectrum. The double-humped structure around 65 keV could be best fitted by the GEANT3 [23] simulation (superimposed magenta color curve) of 65-keV photons emitted by a heavy fission fragment moving with a relatively slow speed of  $\approx 0.025c$ , implying

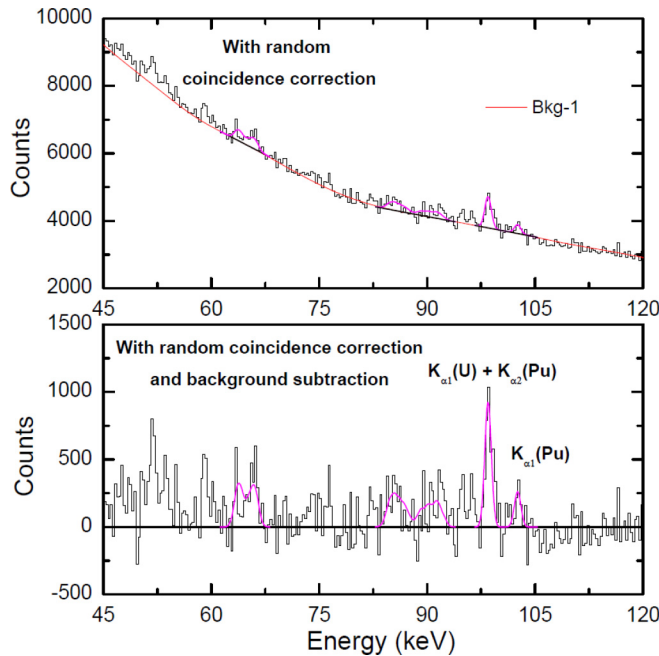


FIG. 5. Random coincidence corrected photon spectrum with Bkg-1 (solid red) background is shown in the upper panel. Bkg-1 subtracted coincidence spectrum is shown in the lower panel. GEANT3 simulations of a fission fragment  $K$  x ray at 65 keV and a fission fragment  $\gamma$  ray at 88 keV are shown in magenta color. The peaks at 98.4 keV and around 103 keV are also shown in magenta color.

highly asymmetric mass splits of excited plutonium nuclei. The ratio of the area under the double-humped structure to its statistical error bar is  $>4$ , thus defining the hump with a high ( $>99\%$ ) statistical confidence. Considering the expected very low yield for such asymmetric mass splits of highly excited plutonium, the double-humped structure is likely to be  $K$  x rays from a heavy fragment (possibly iridium). The double-humped structure around 88 keV could be best fitted by the GEANT3 [23] simulation (superimposed magenta color curve) of 88-keV photons emitted by a fission fragment moving with speed  $\approx 0.05c$ , implying approximately symmetric mass splits of highly excited plutonium nuclei and has been interpreted as a fission fragment  $\gamma$  ray. The ratio of the area under the double-humped structure to its statistical error bar is  $>5$ , thus defining the hump with a high ( $>99\%$ ) statistical confidence. All the GEANT3 [23] simulations have been performed using actual experimental geometry.

There is no hint of any narrow peak exactly at the characteristic plutonium  $K_{\alpha 1}$  energy of 103.7 keV. However, a statistically significant narrow peak near 103 keV is seen in the coincidence spectrum (Fig. 5). The magenta color curve shows a Gaussian fit of the data points from 100.8 to 105.3 keV giving a narrow peak at 102.6 keV with  $\text{FWHM} = 1$  keV. The ratio of peak area of this narrow peak to its statistical error is  $\approx 4$ , thus defining the peak with better than 99% statistical confidence. Since the remnant of uranium  $K$  x-ray lines is present in the coincidence spectrum, let us first discuss whether the narrow peak near 103 keV could be the remnant of a  $\gamma$ -ray or x-ray line in random coincidence with the fission fragments and

appearing in the true coincidence spectrum due to the imperfect cancellation of random coincidence events.

We find from the prompt spectrum [Fig. 3 (lower panel)] that the relative efficiency corrected total yield around 103 keV is about 0.13 times that of the uranium  $K_{\alpha 1}$  (98.4 keV) line and about 0.23 times that of the uranium  $K_{\alpha 2}$  (94.65 keV) line, whereas in the random corrected true coincidence spectrum [Fig. 5 (lower panel)] the relative efficiency corrected yield around 103 keV is about 0.32 times that of the 98.4-keV line and 0.72 times that of the 94.65-keV line. Considering the suppression factor of the uranium atomic excitation lines in the true coincidence spectrum compared to their yields in the singles spectrum, the contribution of random coincidence events around 103 keV in the true coincidence spectrum [Fig. 5 (lower panel)] can account for only  $\approx 20\%$  of the Gaussian peak (magenta color) area ( $\text{FWHM} = 1$  keV) centered around 103 keV. So, the peak seen around 103 keV in the random corrected true coincidence spectrum should mostly be photons in true coincidence with the fission fragments.

It is interesting to discuss possible sources of  $\gamma$  rays and x rays near 103 keV that do not involve emission of fission fragments, but could be in random coincidence with the fission fragments. The excited ( $E_X \approx 55$  MeV) plutonium nucleus produced by  ${}^4\text{He} + {}^{238}\text{U}$  fusion reaction could de-excite [24] by sequential emissions of neutrons followed by a cascade of electromagnetic transitions leading to the emission of plutonium  $K$  x rays by the internal conversion process or from the  $K$  vacancies produced during the fusion process. In addition, some of the plutonium isotopes (such as  ${}^{236}\text{Pu}$ ) could emit 102.8 keV  $\gamma$ -ray photons during the de-excitation process [25]. Coulomb and inelastic excitations of  ${}^{238}\text{U}$  by  ${}^4\text{He} + {}^{238}\text{U}$  reaction also produce 103.5-keV  $\gamma$ -ray photons [26]. Remnants of these events could remain in the random subtracted photon spectrum. Let us discuss all these possibilities one by one.

The Coulomb excitation of  $\gamma$ -ray line of  ${}^{238}\text{U}$  almost overlaps with the plutonium  $K_{\alpha 1}$  line and so their relative intensities cannot be determined from the singles LEPS spectrum. Since the Coulomb excitation line of  ${}^{232}\text{Th}$  is at 112.75 keV [27] and well separated from the thorium atomic excitation lines (93.3 and 89.9 keV), we also obtained singles LEPS spectrum (Fig. 6) from  ${}^4\text{He} + {}^{232}\text{Th}$  reaction at  $E_{\text{LAB}}({}^4\text{He}) = 60$  MeV and found that the yield of Coulomb excitation line is negligible compared to the yields of the atomic excitation lines of thorium. The  $K$  x-ray cross section for  ${}^4\text{He} + {}^{238}\text{U}$  is expected to be  $\approx (20\text{--}30\%)$  lower [28] than that for  ${}^4\text{He} + {}^{232}\text{Th}$  at the same  ${}^4\text{He}$  bombarding energy [ $E({}^4\text{He})_{\text{lab}} = 60$  MeV]. On the other hand, since the internal conversion coefficient of the 162.1-keV,  $4^+$  state of  ${}^{232}\text{Th}$  is 6.8 whereas that of the corresponding 148.4-keV  $4^+$  state of  ${}^{238}\text{U}$  is 11.6 [29], the intensity of Coulomb excitation line of  ${}^{238}\text{U}$  would be lowered considerably compared to that for  ${}^{232}\text{Th}$ . Both  ${}^{232}\text{Th}$  and  ${}^{238}\text{U}$  have similar rotational spectra. The feeding patterns to the  $4^+$  state from upper levels are not very different for the two nuclei. So qualitatively speaking, the ratio of the intensities of Coulomb excitation line to the atomic  $K$  x-ray line should be similar for  ${}^{232}\text{Th}$  and  ${}^{238}\text{U}$  at the same  ${}^4\text{He}$  bombarding energy. Hence, the yield of Coulomb excitation line of  ${}^{238}\text{U}$  at 103.5 keV is expected to be several orders of magnitude

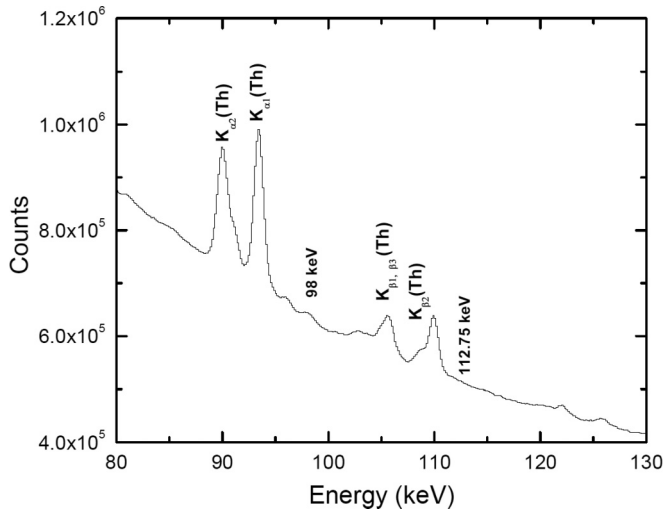


FIG. 6. Singles LEPS detector spectrum of  ${}^4\text{He} + {}^{232}\text{Th}$  reaction at  $E_{\text{LAB}}({}^4\text{He}) = 60$  MeV.

lower than the yield of the atomic excitation line of uranium at 98.4 keV and should not be seen in the true coincidence spectrum. Hence, the sharp peak seen around 103 keV is very unlikely to be the remnant of the Coulomb excitation line. In Ref. [24],  ${}^4\text{He} + \text{Pb}$  and  ${}^4\text{He} + \text{Au}$  reactions were studied at  $E({}^4\text{He})_{\text{Lab}} = 40$  MeV and  $K$  x-ray lines corresponding to Po and Tl produced by the fusion reactions were seen. These were attributed to the compound nucleus emitting neutrons followed by a cascade of  $\gamma$  rays leading to the emission of the corresponding  $K$  x rays. Such a process appears to be present in the  ${}^4\text{He} + {}^{232}\text{Th}$  reaction at  $E({}^4\text{He})_{\text{Lab}} = 60$  MeV, since a 98-keV uranium  $K_{\alpha 1}$  line is seen in the singles spectrum (Fig. 6). It would be very difficult to see a weak uranium  $K_{\alpha 2}$  line in the singles spectrum, as the weak line would overlap with the tail of the very strong thorium  $K_{\alpha 1}$  line. A similar process could be present for a  ${}^4\text{He} + {}^{238}\text{U}$  reaction and in fact, a peak at 103.7 keV has been seen in the singles spectrum. However, these 103.7-keV  $K$  x rays would not be in true coincidence with the fission fragments, although they could contribute to the coincidence spectrum because of imperfect cancellation of random events. Considering the very low yield of such a process in comparison to the atomic excitation lines in the singles spectrum, this process should not produce significant background in the coincidence spectrum. The yield of  ${}^{236}\text{Pu}$  produced by six sequential neutron emissions from the initially produced  ${}^{242}\text{Pu}$  compound nucleus is expected to be very low and the corresponding yield of a 102.8-keV line should be several orders of magnitude smaller than the yields of the atomic excitation lines. So the contribution of a 102.8-keV line from  ${}^{236}\text{Pu}$  would be negligible in the coincidence spectrum. The predominant source of background is fission fragment  $\gamma$  rays in true coincidence with the fission fragments.

#### *a. Fission fragment $\gamma$ -ray versus plutonium $K$ x-ray lines.*

We discuss whether the observed narrow peak near 103 keV is the plutonium ion's  $K_{\alpha 1}$  line with its associated  $K_{\alpha 2}$  line overlapping with the uranium  $K_{\alpha 1}$  line or a fission fragment  $\gamma$ -ray peak whose higher energy hump is around 103 keV

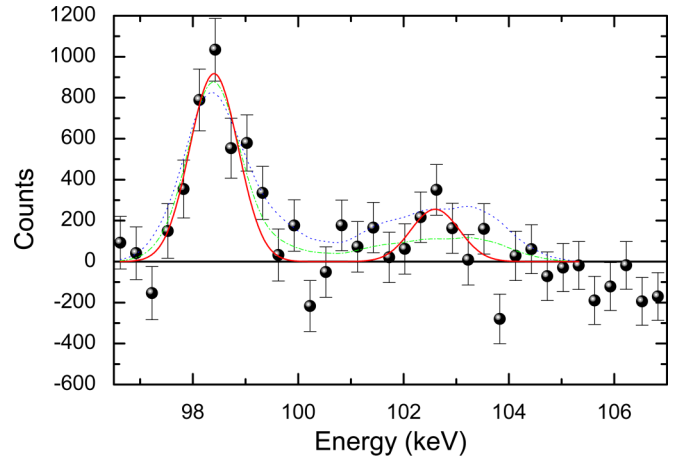


FIG. 7. Random corrected coincidence spectrum for Bkg-1 subtraction with statistical error bars shown in the energy range between 96.6 and 107 keV. Dashed blue and dot-dashed green curves represent GEANT3 simulation of a sharp 101-keV  $\gamma$ -ray line from a fission fragment with additional yield at 98.4 keV. The solid red curve shows Gaussian fit of the data points with two isolated peaks (see text for details).

and the corresponding lower energy hump is overlapping with the uranium  $K_{\alpha 1}$  line. In Fig. 7, we show Bkg-1 subtracted true coincidence spectrum in the energy range from 96.6 to 107 keV with statistical error bars on the data points. Highly excited plutonium nuclei produced in this reaction are most likely to fission into two symmetric mass fragments that move with speed  $\approx 0.04c$ , according to Viola systematic [30]. Considering the case of a fission fragment  $\gamma$  ray, GEANT3 simulation [23] of a sharp 101-keV  $\gamma$ -ray line from a fission fragment corresponding to symmetric mass splits of plutonium nuclei produces a high and a low energy hump around 103 and 98.4 keV respectively. However, GEANT3 simulation of a  $\gamma$ -ray line alone cannot fit the data points in the region from 96.6 to 105.3 keV, because of the presence of an additional 98.4-keV uranium  $K_{\alpha 1}$  line due to the imperfect cancellation of random coincidence events. It is possible to obtain a good fit of the data points (96.6–105.3-keV region) in the coincidence spectrum (Fig. 7) by a combination of GEANT3 simulation of a 101-keV fission fragment  $\gamma$  ray and an additional uranium  $K_{\alpha 1}$  line. We have fitted by two methods. In the first method, at first a GEANT3 simulated curve was adjusted to obtain the best reduced  $\chi^2$ . Then an additional uranium  $K_{\alpha 1}$  Gaussian peak with FWHM = 1 keV was added and the peak area was adjusted to obtain the best possible fit as shown by the dashed blue curve in Fig. 7. This best possible fit gives a reduced  $\chi^2 = 1.64$ . In the second method, both the areas under the GEANT3 simulated curve and the added uranium  $K_{\alpha 1}$  peak were adjusted simultaneously to obtain the best fit (reduced  $\chi^2 = 1.2$ ) as shown by the dot-dashed green curve in Fig. 7. However, in this fit, the area under the double-humped fission fragment peak becomes statistically poorly defined (ratio of area under the GEANT3 simulated curve to its statistical error bar  $\approx 2$ ). We have performed these simulations assuming different speeds of the fission fragment in the range from  $0.035c$  to  $0.05c$ , corresponding to somewhat asymmetric fission events.

In all the cases, we find that the broad fission fragment  $\gamma$ -ray hump is statistically poorly defined.

Let us now consider whether the observed peak around 103 keV could be the plutonium  $K_{\alpha 1}$  line in true coincidence with the fission fragments. The plutonium  $K_{\alpha 1}$  line should be associated with its  $K_{\alpha 2}$  line that would overlap with the uranium  $K_{\alpha 1}$  line. In this case also, we have to add an additional contribution from uranium  $K_{\alpha 1}$  peak due to the imperfect cancellation of random coincidence events. So we fit the data points in the region from 96.6 to 105.3 keV by two isolated Gaussian peaks with peak positions at 102.6 and 98.4 keV (FWHM = 1 keV) as shown by the red curve in Fig. 7 and get an excellent fit with reduced  $\chi^2 = 1.0$ . The ratio of the Gaussian peak area at 102.6 keV to its statistical error bar is  $\approx 4$ , implying that the peak is defined with  $>99\%$  confidence level. So in the scenario of two isolated Gaussian peaks corresponding to plutonium  $K_{\alpha 1}$  and  $K_{\alpha 2}$  lines, we obtain a very good fit of the data points with a high statistical significance for the peaks. Subtracting out the expected yield of plutonium  $K_{\alpha 2}$  peak from the total Gaussian peak area around 98.4 keV, the remaining yield at 98.4 keV should be the remnant of uranium  $K_{\alpha 1}$  line and tally with the observed remnant of uranium  $K_{\alpha 2}$  line at 94.6 keV. We find that the ratio of the relative efficiency corrected yield of the remnants of uranium  $K_{\alpha 2}$  to uranium  $K_{\alpha 1}$  line is  $0.52 \pm 0.17$ , in satisfactory agreement with the known branching ratio of 0.625 [29].

Hence, the description of the data points (96.6–105.3 keV) with a GEANT3 simulated fission fragment  $\gamma$  ray and 98.4-keV remnant uranium  $K_{\alpha 1}$  line either gives an overall poor fit (dotted blue curve) or the best fitted extracted hump (dot-dashed green curve) of the fission fragment  $\gamma$  ray around 103 keV becomes statistically poorly defined. On the other hand, the data points can be fitted very well (red curve) with a high statistical significance by two isolated narrow (FWHM = 1 keV) Gaussian peaks corresponding to plutonium  $K$  x-ray lines and a 98.4-keV remnant uranium  $K_{\alpha 1}$  line.

In the case of a double-humped fission fragment  $\gamma$ -ray spectrum around 88 keV, we get a very good fit (reduced  $\chi^2 \approx 1$ ) of the spectral shape by GEANT3 simulations of the corresponding fission fragment  $\gamma$  ray, assuming the average speed of  $\gamma$ -ray emitting fission fragment  $\approx 0.05c$ . It implies approximately symmetric mass splits of the plutonium nuclei. The broad fission fragment  $\gamma$ -ray hump around 88 keV is defined with a high ( $>99\%$ ) statistical confidence (the ratio of the area under the hump to its statistical error bar is  $>5$ ). On the other hand, a single narrow Gaussian peak cannot provide any reasonable fit (typical reduced  $\chi^2 \approx 2$ ) of either hump around 88 keV. So, clearly, the spectral shape around 103 keV is qualitatively different from the spectral shape of the 88-keV fission fragment  $\gamma$  ray, indicating that the photons seen around 103 keV is unlikely to be from a fission fragment  $\gamma$  ray.

We have performed another statistical test to determine whether the data points in the 100.8–105.3-keV region indicate the presence of a narrow Gaussian peak around 103 keV or the high energy hump of a fission fragment  $\gamma$  ray. In Fig. 8, we show the coincidence photon spectrum from 100.5 to 105.9 keV with statistical error bars. The dot-dashed green curve is the high energy hump of GEANT3 simulation for a 101-keV sharp fission fragment  $\gamma$ -ray line as discussed

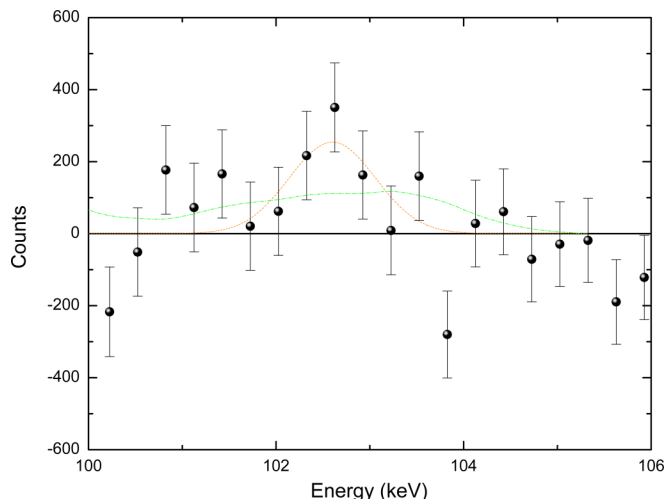


FIG. 8. Random corrected coincidence spectrum for Bkg-1 subtraction with statistical error bars in the energy range from 100.5 to 105.9 keV. Dot-dashed green curve is the high energy hump for best fitted GEANT3 simulation of 101-keV fission fragment  $\gamma$ -ray. Dotted red curve is the best fit for a combination of GEANT3 simulation of fission fragment  $\gamma$  ray and a Gaussian peak around 103 keV with FWHM = 1 keV as discussed in the text.

before. Let us now assume that a narrow Gaussian peak (FWHM = 1 keV) around 103 keV is also present in addition to the GEANT3 simulated hump. So we fit the data points with a combination of GEANT3 simulated hump and a narrow Gaussian peak and adjust the areas of the Gaussian peak and GEANT3 simulated hump to obtain the best fit of the data points as shown by the dotted red curve of Fig. 8. The best fit (dotted red curve) dramatically suppresses the contribution from a GEANT3 simulated hump and prominently projects out the Gaussian peak, implying that a narrow Gaussian peak is statistically a much better description of the data points than a Doppler broadened fission fragment  $\gamma$ -ray hump.

Another method to distinguish between a fission fragment  $\gamma$  ray and  $K$  x ray from the element produced by nuclear fusion could be to determine photon multiplicities at the relevant photon energies by gating on different regions of the fission fragment energy spectrum as discussed before. We have divided the fission fragment kinetic energy spectrum into three parts and each part contains the same number of fission fragments. On the average, the fission fragments in the low (0–75 MeV) and high (98–220 MeV) fission fragment kinetic energy regions should be coming from asymmetric mass splits of the highly excited fissioning plutonium nuclei, whereas the fission fragments in the central kinetic energy region (75–98 MeV) should be coming from approximately symmetric mass splits of the fissioning nuclei. In Fig. 9, we show measured photon multiplicities of the 103-, 88-, and 65-keV peaks as obtained by gating on different regions of the fission fragment kinetic energy spectrum. The horizontal bar on each data point indicates the fission fragment kinetic energy region over which the gating has been done. The photon multiplicity is the ratio of photon cross section at the relevant energy and total fission cross section. The photon cross section is proportional to the measured photon yield and the method of

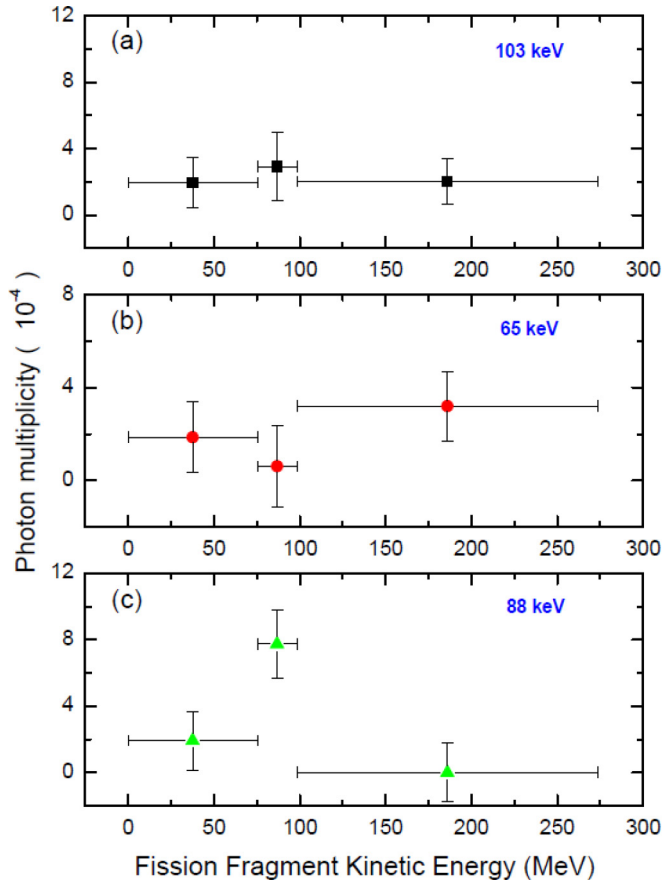


FIG. 9. Photon multiplicities of the 103-keV [panel (a)], 88-keV [panel (c)], and 65-keV [panel (b)] peaks as obtained by gating on different regions of fission fragment energy spectrum. The horizontal error bar on each data point indicates the regions of the fission fragment kinetic energy spectrum over which gating has been done.

obtaining a photon cross section from the normalized photon yield is described in a later subsection. The total fission cross section has been taken as 2 barns from Jain *et al.*'s measurement [31]. We have suggested from the GEANT3 simulation fit shown in Fig. 5 that the 65-keV structure is due to  $K$  x-ray photons from a fission fragment moving with speed  $\approx 0.025c$ , implying very asymmetric mass splits of the highly excited plutonium nuclei. In Fig. 9(b), we expect that the yield of a 65-keV x ray should be equally distributed between the low and high fission fragment kinetic energy bins and it should be the lowest and consistent with zero in the central fission fragment kinetic energy bin. However, the uncertainties on the data points [Fig. 9(b)] are too large to reach any conclusion. In Fig. 9(a), we find that almost all the yield of the 88-keV  $\gamma$  ray is coming from the central fission fragment kinetic energy bin, qualitatively supporting the GEANT3 simulation result that the origin of the 88-keV  $\gamma$  ray should be from approximately symmetric mass splits of the fissioning nuclei. Let us now discuss what we expect if a 101-keV fission fragment  $\gamma$  ray is producing the observed spectral shape in the 96.6–105.3-keV region. The fit of the spectral shape with the GEANT3 simulation of 101-keV fission fragment  $\gamma$  ray indicates that the speed of the corresponding fission fragment should be  $\approx 0.04c$ , implying

symmetric mass splitting of the plutonium nucleus. If it is a fission fragment  $\gamma$  ray, the relatively high multiplicity of the 101-keV peak is also indicative of its origin from symmetric mass splitting. So, qualitatively speaking, the multiplicity plots (Fig. 9) for both the 88- and 101-keV fission fragment  $\gamma$  rays should be similar and hence, almost all the yield of the 101-keV fission fragment  $\gamma$  ray is expected to be in the central fission fragment kinetic energy bin. The qualitative observation of about equal photon multiplicity in all fission fragment kinetic energy bins [Fig. 9(a)] implies that the origin of the photons around 103 keV cannot be related to a  $\gamma$  ray from any fission fragment and is likely to be  $K$  x-ray photons from a heavy element, in agreement with our earlier conclusion from the spectral shape.

*b. Evidence in favor of plutonium  $K_{\alpha 1}$  line.* We find from Fig. 8 that the spectral shape in the 100.5–105.3-keV region is best fitted by a single narrow Gaussian function (FWHM  $\approx 1$  keV) peaked around 103 keV with a high statistical confidence level without requiring any Doppler broadening. The counts under the narrow peak at 103 keV are about five times larger than the estimated random coincidence counts. In Fig. 9, we find that the photon multiplicity of the narrow 103-keV peak remains about the same in all the three fission fragment kinetic energy bins. These observations provide evidence that the photon peak around 103 keV is coming from a heavy element that undergoes fission to produce the fission fragments detected in coincidence by the photovoltaic cell detector assembly. Since low energy  $\gamma$ -ray ( $\sim 100$  keV) emission from the highly excited plutonium nucleus ( $E_X \approx 55$  MeV) cannot compete with the neutron emission and fission decay [9,20,29], the observed photon peak around 103 keV must be a  $K$  x-ray line from a heavy element ( $Z > 92$ ). Since the cross section for the production of neptunium ( $Z = 93$ ) is expected to be very small, the only possibility is that it should be the plutonium  $K_{\alpha 1}$  line and the corresponding  $K_{\alpha 2}$  line is overlapping with the uranium  $K_{\alpha 1}$  line. So, we are interpreting this high energy photon line around 103 keV as the plutonium  $K_{\alpha 1}$  line.

*c. Gaussian peak fitting and determination of fission time of slow fission events.* In Fig. 7, we have shown by the red curve the best Gaussian fit of the data points from 101.7 to 103.5 keV. The Gaussian fit gives a peak position at 102.6 keV with FWHM =  $(1 \pm 0.3)$  keV. The energy resolution (FWHM) of LEPS detector for uranium  $K_{\alpha 1}$  line (98.4 keV) as obtained from the singles LEPS spectrum is  $(1.00 \pm 0.01)$  keV. Since the plutonium  $K_{\alpha 2}$  line is expected to merge with the uranium  $K_{\alpha 1}$  line (98.4 keV), we have determined from a double Gaussian fit of the data points around 98.4 keV that the FWHM of the plutonium  $K_{\alpha 2}$  line is  $(1 \pm 0.4)$  keV. Thus by combining Gaussian analyses of the peaks at 102.6 and 98.4 keV, we obtain that the FWHM of plutonium ion's  $K$  x-ray line in coincidence with the fission fragments is  $(1 \pm 0.24)$  keV. Since the LEPS detector resolution as obtained from the singles spectrum in a beam-on environment is  $(1.00 \pm 0.01)$  keV and the intrinsic width of plutonium  $K$  x-ray line [32] for a neutral plutonium atom with its nucleus at the ground state is 0.1 keV, the increase of the intrinsic width of plutonium  $K$  x-ray line for the fissioning plutonium nucleus is  $(0 \pm 0.24)$  keV. So, the mean fission time of the long-lived fissioning plutonium nuclei responsible for the observed atomic  $K$  x-ray



yield could be estimated [15] as  $> \frac{\hbar}{2.35 \times 0.24 \text{ keV}} = 1 \times 10^{-18} \text{ s}$ . Here  $\hbar = \frac{h}{2\pi}$  and  $h$  is Planck's constant. The fission events with a short fission time  $\approx 10^{-20} \text{ s}$  would produce about 60-keV broad  $K$  x-ray peaks and the corresponding  $K$  x-ray yield would be about two orders of magnitude smaller than that for slow fission events (fission time  $\approx 10^{-18} \text{ s}$ ) for the same number of fission events. Such a broad and weak  $K$  x-ray hump associated with short fission time would be cut out by our background curve. Hence, this method is sensitive to the long fission time component like any other atomic technique [1–6]. We conclude that the fission time of slow fission events producing the observed plutonium  $K$  x-ray peak is  $> 1 \times 10^{-18} \text{ s}$ . However, it is not possible to determine the percentage of slow fission events only from the analysis of the peak width.

*d. Determination of percentage of slow fission events.* In order to determine the minimum percentage of slow fission events produced in the reaction we have assumed an extreme bimodal fission time distribution with a very long-lived fission component ( $\tau_f \rightarrow \infty$ ) and a very short-lived fission component ( $\tau_f \rightarrow 0$ ) that does not contribute at all to  $K$  x-ray yield. Then the percentage of slow fission events corresponding to this extreme bimodal fission time distribution is given by  $f_L = \frac{\sigma_K}{P_K \sigma_f} \times 100\%$  [14], where  $\sigma_K$  is the  $K$  x-ray cross section of the plutonium ions produced in the fusion reaction and whose nuclei would fission,  $\sigma_f$  is the fission cross section, and  $P_K$  is the probability of creation of  $K$  vacancies of plutonium produced in the fusion reaction. Any other fission time distribution would produce a higher percentage of slow fission events [14]. The absolute fission cross section ( $\sigma_f$ ) of plutonium produced by the  ${}^4\text{He} + {}^{238}\text{U}$  reaction at  $E_{\text{LAB}}({}^4\text{He}) = 60 \text{ MeV}$  was measured by Jain *et al.* [31] and found to be  $\sigma_f = (2 \pm 0.1)$  barns. The absolute plutonium  $K$  x-ray cross section ( $\sigma_K$ ) has been estimated by the method described below and then the quantity ( $\sigma_K/\sigma_f$ ) has been computed.

*(i) Determination of  $\sigma_K/\sigma_f$ .* Kravchuk *et al.* [33] measured the absolute  $K$  x-ray cross section for  ${}^4\text{He} + {}^{181}\text{Ta}$ ,  ${}^4\text{He} + {}^{208}\text{Pb}$ , and  ${}^4\text{He} + {}^{232}\text{Th}$  at  $E_{\text{Lab}}({}^4\text{He}) = 80 \text{ MeV}$  with  $\approx 10\%$  uncertainty and compared with KXCROSS code calculations obtaining reasonable agreement between theory and experiment within two standard deviations or better. The data points [33] for  ${}^4\text{He}$  induced reaction fall on a straight line when plotted as the reduced velocity versus reduced  $K$  x-ray cross section. The reduced velocity is given by  $\xi_K = \frac{2v_p}{\theta v_K}$ , where  $v_p$  is the speed of the projectile and  $v_K$  is the speed of the  $K$  orbital electron of target and  $\theta = \frac{E_B}{(Z_T - 0.3)^2 R}$  where  $E_B$  is the binding energy of the  $K$  orbital for the target,  $Z_T$  is the atomic number of the target atom, and  $R = 13.6 \text{ eV}$  is the Rydberg constant. The reduced  $K$  x-ray cross section is  $\sigma_X/Z_p^2$ , where  $Z_p$  is the atomic number of the projectile and  $\sigma_X$  is the absolute  $K$  x-ray cross section. In the case of the  ${}^4\text{He} + {}^{238}\text{U}$  reaction at  $E_{\text{LAB}}({}^4\text{He}) = 60 \text{ MeV}$ ,  $\xi_K = 0.54$ . So, the fitted straight line as obtained from Ref. [33] was extrapolated slightly to obtain the absolute  $K$  x-ray cross section  $\sigma_X = 1.7$  barns, corresponding to  $\xi_K = 0.54$ . Since the uncertainties on all the measured  $K$  x-ray cross sections were about 10% and they (experimental data points for  ${}^4\text{He}$  on heavy elements) agree with KXCROSS code calculations within two standard deviations or better [33], the uncertainty on the absolute  $K$  x-ray cross section

for  ${}^4\text{He} + {}^{238}\text{U}$  at  $E_{\text{LAB}}({}^4\text{He}) = 60 \text{ MeV}$  could be expected to be  $\sim 20\%$ . We have done a cross check for the absolute  $K$  x-ray cross section of  ${}^4\text{He} + {}^{238}\text{U}$  at  $E_{\text{LAB}}({}^4\text{He}) = 60 \text{ MeV}$  in another way. Kravchuk *et al.* [33] measured a  $K$  x-ray cross section = 3.3 barns within 10% uncertainty for  ${}^4\text{He} + {}^{232}\text{Th}$  at  $[E_{\text{Lab}}({}^4\text{He}) = 80 \text{ MeV}]$ . In Ref. [28],  $K$  x-ray cross sections for  ${}^4\text{He}$  on different heavy elements at different energies have been tabulated. These are much older results with  $\sim 30\%$  error bars. The absolute cross sections from these older compilations [28] are generally lower than those obtained by Kravchuk *et al.* [33], but they almost agree within error bars. The ratio of the corresponding  $K$  x-ray cross sections obtained from Refs. [33] and [28] agree reasonably well. Using the measured  $K$  x-ray cross section [33] of  ${}^4\text{He} + {}^{232}\text{Th}$  at  $[E_{\text{Lab}}({}^4\text{He}) = 80 \text{ MeV}]$  and the relevant ratios of  $K$  x-ray cross sections obtained from Ref. [28], we obtain a  $K$  x-ray cross section ( $\approx 1.5$  barns) for  ${}^4\text{He} + {}^{238}\text{U}$  at  $E_{\text{LAB}}({}^4\text{He}) = 60 \text{ MeV}$ , in reasonable agreement with our earlier result of 1.7 barns. Using the known branching ratio of the  $K_{\alpha 1}$  line for uranium, the absolute cross section of the uranium  $K_{\alpha 1}$  line is  $(\sigma_{\text{UK}\alpha 1})_{\text{singles}} \approx 0.8$  barn for the  ${}^4\text{He} + {}^{238}\text{U}$  reaction at  $E_{\text{LAB}}({}^4\text{He}) = 60 \text{ MeV}$  and the uncertainty on the cross section could be taken as  $\sim 20\%$ .

The observed plutonium  $K_{\alpha 1}$  yield (as obtained from the Gaussian fitting of the 102.6-keV peak in Fig. 7) could still contain some random coincidence events due to the imperfect cancellation of the background lines in the coincidence spectrum and so another correction factor was applied. This correction factor has been obtained by dividing the remnant yield of  $K_{\alpha 2}$  (94.65 keV) observed in the coincidence spectrum with the corresponding yield in the singles photon spectrum and the correction factor has been assumed to be the same at 98 and 103 keV. The correction factor reduced the yield of the Gaussian area at 102.6 keV by  $\approx 20\%$ . Let  $N_{103}$  be the corrected true coincidence yield of the plutonium ion's  $K_{\alpha 1}$  line in coincidence with the fission fragments and  $N_{98}$  be the yield of the 98.4-keV uranium  $K_{\alpha 1}$  line in the singles LEPS spectrum. Let  $\epsilon_f$  be the efficiency of the fission detector. Let  $\epsilon_{98}$  and  $\epsilon_{103}$  be the efficiencies of the LEPS at 98.4 and 103 keV. Then normalizing with respect to the yield of the 98.4-keV uranium  $K_{\alpha 1}$  line measured simultaneously by the same LEPS in the singles spectrum, we obtain the cross section of the  $K_{\alpha 1}$  line of the plutonium ions (whose nuclei would undergo fission) as  $(\sigma_{\text{PuK}\alpha 1})_{\text{coincidence}} = \frac{(\sigma_{\text{UK}\alpha 1})_{\text{singles}} \times N_{103} \times \epsilon_{98}}{N_{98} \times \epsilon_f \times \epsilon_{103}}$ , where  $(\sigma_{\text{UK}\alpha 1})_{\text{singles}}$  is the cross section of uranium  $K_{\alpha 1}$  line and  $(\sigma_{\text{UK}\alpha 1})_{\text{singles}} \approx 0.8$  barn as obtained earlier. The ratio  $(\epsilon_{98}/\epsilon_{103})$  is the relative efficiency of LEPS for the 98.4-keV line with respect to 103 keV and was obtained from our measured relative efficiency curve of the LEPS. The efficiency of the fission detector ( $\epsilon_f$ ) was obtained from the actual geometry of the fission detector using GEANT3 simulation code [23]. Hence the cross section  $(\sigma_{\text{PuK}\alpha 1})_{\text{coincidence}}$  was obtained and it was corrected by the known branching ratios [29] of plutonium  $K$  x rays to obtain total  $K$  x-ray cross section ( $\sigma_K$ ) of plutonium ions whose nuclei would undergo fission. Thus, we obtain  $\sigma_K/\sigma_f = 5.6 \times 10^{-4}$  with  $\sim 35\%$  uncertainty. The uncertainty mostly comes from the statistical uncertainty on  $N_{103}$ . A cross check was done by estimating this ratio ( $\sigma_K/\sigma_f$ ) from the known target thickness, number of incident beam particles, fission cross section of

plutonium, measured plutonium  $K$  x-ray yield, and coincidence efficiency and we obtained  $\sigma_K/\sigma_f \approx 7 \times 10^{-4}$  with  $\sim 50\%$  uncertainty. So the two methods of estimating ( $\sigma_K/\sigma_f$ ) agree within the error bars.

(ii) *Determination of  $P_K$  (probability of creating  $K$  vacancy in plutonium).* In order to determine the slow fission component, we also need to know the probability ( $P_K$ ) of creating a  $K$  vacancy in plutonium due to the  ${}^4\text{He} + {}^{238}\text{U}$  fusion reaction at  $E_{\text{LAB}}({}^4\text{He}) = 60$  MeV, and this is discussed below.

Kravchuk *et al.* [34] compiled  $K$  orbital ionization probabilities ( $P_K$ ) of different targets (such as Pb, Th, etc.) due to the collisions with  ${}^4\text{He}$  ions of different energies ranging from 25 to 75 MeV for a zero impact parameter (atomic scale). They plotted reduced velocity  $\xi_K$  (as defined before) versus  $P_K/Z^2$  (where  $Z$  is the atomic number of the target atom) for various targets and energies and the data points could be approximated [34] by a theoretical curve. Hence, irrespective of the target used, the value of  $P_K/Z^2$  for any specific reduced velocity could be obtained from this curve. Using the curve given by Kravchuk *et al.* [34], we find that at  $\xi_K = 0.54$ , the probability of  $K$  orbital ionization of  ${}^{238}\text{U}$  is  $P_{\text{el}} = 5.3 \times 10^{-4}$ . Since the data points near  $\xi_K = 0.54$  are about 20–25% below the theoretical curve [34], we assign an error bar of  $\approx 25\%$  on  $P_{\text{el}}$ . Since only the incoming part of the trajectory must be taken into account in the case of fusion, the probability of creation of a  $K$  orbital vacancy in uranium due to the interaction with  ${}^4\text{He}$  of 60-MeV energy could be approximately taken [6] as  $P_{\text{el}}/2 = (2.65 \pm 0.66) \times 10^{-4}$ . As  ${}^4\text{He}$  would fuse with  ${}^{238}\text{U}$  to produce  ${}^{242}\text{Pu}$ , essentially all the  $K$  orbital vacancies of uranium produced from the incoming trajectory would be transferred to the plutonium and significantly more  $K$  orbital vacancies would be produced by the shakeoff process.

As  ${}^4\text{He}$  comes within the nuclear interaction region of  ${}^{238}\text{U}$ , we assume that fusion immediately takes place in a time scale much shorter than the electronic rearrangement time causing shakeoff ionization. Following Carlson *et al.*'s treatment [35], we use the sudden approximation to calculate the probability of  $K$  orbital ionization of plutonium due to the shakeoff process. In the case of the single ionization of the  $K$  orbital of plutonium, one electron of the  $1s$  orbital of uranium would go to the  $1s$  orbital of the newly created plutonium and the other electron would go elsewhere. Since the overlap of  $1s$  orbitals of uranium and plutonium is very close to 1, the probability of single ionization of the plutonium  $K$  orbital due to the shakeoff process [ $P_K(\text{shakeoff})$ ] is essentially equal to the probability that one electron of the  $1s$  orbital of uranium would not go to the  $1s$  orbital of the newly created plutonium ion. Hence, in the sudden approximation,  $P_K(\text{shakeoff}) = 1 - |\int_V \psi_{\text{Pu}}^*(1s)\psi_{\text{U}}(1s)dV|^2$  where  $\psi_{\text{U}}(1s)$  and  $\psi_{\text{Pu}}(1s)$  are the  $1s$  electronic wave functions of uranium and plutonium atoms respectively and the integral is over the entire volume. Carlson *et al.* [35] found that for high  $Z$  atoms, wave functions obtained from self-consistent field theories (such as Hartree-Fock) gave much better agreement with the beta decay experimental results than the hydrogenic wave functions. It was found [35] that in the case of  $\beta$  decays from uraniumlike nuclei, the square of the overlap integral of the corresponding  $1s$  orbital atomic wave functions as obtained from the self-consistent

field theory had been about 0.01% smaller than hydrogenic wave functions. Using hydrogenic wave functions, we obtain  $|\int_V \psi_{\text{Pu}}^*(1s)\psi_{\text{U}}(1s)dV|^2 = 0.9996531$ . Reducing it by 0.01%, we obtain  $P_K(\text{shakeoff}) = 0.00045$ . In the case of the overlap integral between plutonium and uranium wave functions, the reduction factor could be somewhat larger than 0.01%, but that has not been considered. So,  $P_K(\text{shakeoff}) \geq 0.00045$ . Hence, the total probability of creating a  $K$  orbital vacancy in plutonium due to the fusion of 60 MeV  ${}^4\text{He}$  with  ${}^{238}\text{U}$  is  $P_K = \frac{P_{\text{el}}}{2} + P_K(\text{shakeoff}) \geq 7.2 \times 10^{-4}$ . The value of  $P_{\text{el}}$  is known within  $\approx 25\%$  as discussed before. Our uncertainty on  $P_K$  is primarily coming from our model calculation for shakeoff ionization using the sudden approximation [35]. Since there are no experimental data for shakeoff ionization produced by fusion reaction, we have not been able to do any independent check on our model calculation. However, this method has been very successful [35] to calculate shakeoff ionization produced during  $\beta$ -particle emission. Recently Sharma and Nandi [36] applied sudden approximation to consider the effect of nuclear recoil due to the sudden onset of nuclear potential near the interaction barrier and calculated the probability of shakeoff ionization of the outer electronic orbitals of projectile ions ( ${}^{56}\text{Fe}$ ,  ${}^{58}\text{Ni}$ , and  ${}^{63}\text{Cu}$ ) bombarding a  ${}^{12}\text{C}$  target near Coulomb barrier energy. So, the method of sudden approximation should be applicable for fusion reaction to calculate the shakeoff ionization probability of the  $K$  orbital [ $P_K(\text{shakeoff})$ ].

Taking the probability of creation of  $K$ -orbital vacancy  $P_K = 7.2 \times 10^{-4}$ , we obtain  $f_L = \frac{\sigma_K}{P_K \sigma_f} \times 100\% = 78\%$  for the extreme bimodal fission time distribution. Hence, the minimum percentage of slow fission events is 78% and for any other fission time distribution,  $f_L$  would increase. Assuming a single average fission time ( $\tau_f$ ) for all the fission events and taking the  $K$  vacancy lifetime of plutonium ( $\tau_{Kx}) = 6 \times 10^{-18}$  s [29], we obtain [5]

$$\tau_f = \frac{\tau_{Kx}}{P_K \left( \frac{\sigma_f}{\sigma_K} \right) - 1} = 2 \times 10^{-17} \text{ s},$$

in agreement with the fission time  $\tau_f > 1 \times 10^{-18}$  s obtained earlier from the increase of the intrinsic width of plutonium  $K$  x-ray lines. However, it should be noted that the fission time determined by the  $K$  x-ray technique is essentially the average fission time of long-lived slow fission events, as discussed before. In our estimate of the minimum percentage of slow fission events, we have used the lower limit of  $P_K(\text{shakeoff})$  as obtained from our model calculation. A higher value of  $P_K$  corresponds to a lower value of  $f_L$  and shorter  $\tau_f$ . Since we know from the width of plutonium  $K$  x-ray lines that  $\tau_f > 1 \times 10^{-18}$  s, we obtain an upper limit for  $P_K$  ( $P_K < 36 \times 10^{-4}$ ) from the formula

$$P_K = \left( \frac{\sigma_K}{\sigma_f} \right) \left[ 1 + \frac{\tau_{Kx}}{\tau_f} \right].$$

Considering this upper limit, i.e.,  $P_K = 36 \times 10^{-4}$ , we obtain  $f_L = 15.6\%$  for the extreme bimodal fission time distribution. However, the lifetime of long-lived fission component is infinity for the extreme bimodal fission time distribution. Assuming that the lifetime of long-lived fission component is not longer than  $10^{-18}$  s, all (100%) the fission events must be long-lived

( $\tau_f = 1 \times 10^{-18}$  s) to explain the observed plutonium  $K$  x-ray multiplicity per fission event, even for  $P_K = 36 \times 10^{-4}$ . Hence, there is a very strong ground to arrive at the qualitative conclusion that the majority of the fission events would be long-lived for a realistic fission time distribution, in agreement with the earlier results [1,3] obtained from similarly excited uraniumlike nuclei.

*e. Shift of plutonium  $K$  x-ray line.* The centroid of the peak around 103 keV (interpreted as the plutonium  $K_{\alpha 1}$  line) has been obtained by taking the weighted average of the channel counts over the Gaussian peak and tail region and found to be  $(102.8 \pm 0.5)$  keV. The statistical uncertainty of the centroid position primarily comes from the uncertainties of the data points in the tail region of the peak. The counts of the data points in the tail region are small. However their uncertainties remain substantial and do not decrease away from the peak position. As a result, the centroid position is about the same as the Gaussian peak position, but the uncertainty on the centroid position is relatively large ( $\pm 0.5$  keV), indicating the possible non-Gaussian shape of the peak. However the uncertainties on the fitting parameters of the Gaussian function (peak position and  $\sigma$ ) remain small, because the contributions to the reduced  $\chi^2$  value from the data points in the tail region are insignificant. Since the energy of a peak is defined by its centroid position, we consider the energy of the peak =  $(102.8 \pm 0.5)$  keV and it agrees with the standard value of the plutonium  $K_{\alpha 1}$  line (103.7 keV) [29] of a neutral plutonium atom within two error bars. If we interpret this peak at  $(102.8 \pm 0.5)$  keV as the plutonium  $K_{\alpha 1}$  line, the corresponding plutonium  $K_{\alpha 2}$  line would be at 98.6 keV overlapping with the uranium  $K_{\alpha 1}$  line. Earlier experiments [1,6] observed very broad  $K$  x-ray bumps in coincidence with the fission fragments and could not obtain precise  $K$  x-ray energies within a fraction of a keV. So our interpretation of assigning plutonium  $K$  x-ray peaks at a slightly lower energy when coming from a plutonium ion containing a highly excited fissioning nucleus does not contradict earlier experimental results.

Carlson *et al.* [35] found from their calculations that a uranium atom should lose about 30% of its outer orbital electrons as a result of sudden emission of a  $\beta$  particle from the atomic nucleus. In the case of plutonium produced by the fusion of  $^4\text{He}$  with  $^{238}\text{U}$ , plutonium should lose significantly more than 30% of its outer orbital electrons. As a result of losing a significant number of outer orbital electrons, the inner  $2p$  electronic orbital would see less screening and  $K$  x-ray energies of plutonium would be lowered. A multielectron atomic calculation [37] using relativistic Dirac equation was carried out and it was found that for xenonlike plutonium,  $K_{\alpha 1}$  and  $K_{\alpha 2}$  x-ray lines would come at 0.03 keV lower energies compared to a neutral plutonium atom.

In the case of very long fission time, the effective Coulomb potential of the rotating prolate shaped fissioning nucleus could reduce the binding energy of the  $1s$  electronic orbital of the plutonium ion and the corresponding  $K$  x-ray energies by a relatively significant amount as we discuss below. It is known [38] that the finite nuclear size correction for the ground state of the uranium nucleus reduces the binding energy of the  $1s$  orbital of the uranium ion by about 0.2 keV. Kozhedub *et al.*

[38] developed a general formalism to calculate eigenstate energies of electronic orbitals considering the effect of nuclear deformation and spin. The Coulomb interaction operator between an atomic electron and the nucleus was averaged with the nuclear wave function and integrated over the nuclear angular variables. Time independent relativistic Dirac equation for the atomic electrons was solved as an eigenvalue problem by using this effective Coulomb potential. Following the procedure of Ref. [38], the effective Coulomb potential of the ground state (spin = 0) of the prolate deformed  $^{242}\text{Pu}$  (semimajor axis =  $a$ , semiminor axis =  $b$ ) nucleus should be obtained by averaging over all the orientations of the nucleus in three dimensions and it would be spherically symmetric. The effective nuclear shape would be a sphere of radius  $b$  with normal nuclear density and the density will drop rapidly for  $r > b$ , thus giving a small effective charge radius. In our experiment,  $^{242}\text{Pu}$  was produced at an excitation energy of  $E_X = 55$  MeV with an average orbital angular momentum  $\approx 20\hbar$  [21] and the orbital angular momentum vector was equally probable to take all possible orientations perpendicular to the beam axis ( $m = 0$  magnetic substrate with respect to the beam axis). Since the nuclear rotation time ( $\approx 10^{-20}$  s) is much shorter compared to the  $K$  x-ray emission time of  $6 \times 10^{-18}$  s, we have assumed an effective Coulomb potential for long fission time scenario and solved the time independent Dirac equation for the electrons as an eigenvalue problem to obtain an order of magnitude estimate of the  $K$  x-ray shift due to the fissioning nucleus. The effective charge radius of the rotating prolate shaped nucleus would increase from the ground state value, as the elongation of the prolate nucleus would increase due to the fission process, thus reducing atomic  $K$  x-ray energies due to the Coulomb effect. A long fission time can be obtained [12,13,39] by increasing the viscosity parameter, thus slowing down the fission process. Combined dynamical and statistical model calculations [39] use a rather weak friction for the compact shape of the fissioning nucleus and the friction increases significantly for large deformation, implying that the fissioning nucleus spends most of its time in saddle to scission configurations. Prefission particle multiplicity data, in general [13,20], give a relatively long saddle to scission time and much shorter presaddle time. However, the nuclear experiments give overall short fission delay time ( $\sim 10^{-20}$  s). On the other hand, long fission time could be obtained [13] by increasing friction inside the saddle and the saddle to scission time contributes only weakly to the long fission time in this model. The results obtained from prefission particle multiplicity data and atomic techniques have not yet been properly reconciled [14] and different models of fission dynamics appear to be contradictory. In order to understand plutonium  $K$  x-ray shift by  $(0.9 \pm 0.5)$  keV, we need to assume that the fissioning plutonium nucleus spends most of its long fission time with a highly deformed dumbbell-type shape. Bulgac *et al.*'s [11] simulations show that the saddle to scission configurations of  $^{240}\text{Pu}$  ( $E_X = 8$  MeV) look approximately dumbbell shaped most of the time. In order to get an order of magnitude estimate of the shift of the  $K$  x-ray line for the rotating dumbbell shaped plutonium nucleus, we have studied the solutions of the time independent Dirac equation for the electrons by increasing the radius of spherical plutonium nucleus assuming uniform nuclear density throughout the

volume. We start with a spherical plutonium nucleus of radius  $1.25 \times (242)^{1/3} \text{ fm} = 7.8 \text{ fm}$ . The corresponding radius for the saddle shape has been taken as 13.2 fm and that of the scission point as 18.9 fm [13]. Considering an intermediate dumbbell-type configuration between saddle and scission corresponding to a spherical plutonium nucleus of radius 15 fm because of the rotation of the dumbbell shaped nucleus in three dimensions, we obtain [37,40] a downward shift of the plutonium  $K$  x-ray line by 0.5 keV compared to a spherical plutonium nucleus of radius 7.8 fm. Since the ground state of a plutonium nucleus would correspond to an even smaller (radius  $< 7.8 \text{ fm}$ ) spherical charge distribution corresponding to the semiminor axis of the ground state prolate nucleus, we expect an additional shift of about 0.06 keV [37]. As discussed before, the electronic shake-off process would produce a xenonlike plutonium and the expected  $K$  x-ray shift would be about 0.03 keV [37] compared to a neutral plutonium atom. So the  $K_{\alpha 1}$  x-ray line of a xenonlike plutonium ion with a spherical nucleus of charge radius 15 fm would be shifted down by about 0.6 keV compared to a neutral plutonium atom with its nucleus at the ground state. This  $K$  x-ray shift would increase to  $> 1 \text{ keV}$  [37] when the fissioning plutonium nucleus would be at the scission point. Different long-lived configurations between the saddle and scission would contribute to the width of the  $K$  x-ray peak and this width would be comparable to its total shift. Our candidate peak is shifted down from the standard plutonium  $K_{\alpha 1}$  x-ray line by  $(0.9 \pm 0.5) \text{ keV}$  and its intrinsic width is  $\leq 0.6 \text{ keV}$ . Hence, in order to be consistent with our order of magnitude estimates, the fissioning plutonium nucleus should spend most of its long fission time with a highly deformed dumbbell-type shape.

*f. No shift scenario.* Let us consider the scenario where the plutonium  $K$  x-ray lines have to appear exactly at the standard positions and the observed shift cannot be attributed to electronic effects. In that case, the observed narrow peak (FWHM  $\approx 1 \text{ keV}$ ) at 102.8 keV has to be considered as an unknown peak or as a part of a broad fission fragment  $\gamma$ -ray peak. However, this latter interpretation is statistically very unlikely as discussed before. No narrow peak has been seen at 103.7 keV in Figs. 4 and 7. Considering the presence of an unknown narrow peak at 102.8 keV or taking the peak at 102.8 keV as a part of a broad fission fragment  $\gamma$ -ray peak, we have attempted to fit a narrow (FWHM = 1 keV) Gaussian peak at 103.7 keV before drawing any background (from Fig. 4) and also after drawing background (from Fig. 7). For extracting the area from Fig. 4, we varied the linear background under the peak to obtain the best possible fit. We obtain average counts under the 103.7-keV peak =  $-271 \pm 284$ . A similar result was obtained for extracting peak area under 103.7-keV peak from Fig. 7. Hence, the corresponding percentage of slow fission events is negligible ( $< 5\%$ ) and contradicts the claims of  $> 70\%$  or almost 100% slow fission events reported earlier in similarly excited uraniumlike nuclei by  $K$  x-ray fluorescence [1] and crystal blocking [3] techniques respectively. Summarizing the two possible alternative scenarios, if the line at 102.8 keV is the plutonium  $K_{\alpha 1}$  line shifted by Coulomb effects, we obtain that most of the fission is slow. If on the other hand, we assume Coulomb effects are negligible, the absence of a peak at the expected energy (103.7 keV) implies that most of the fission is fast.

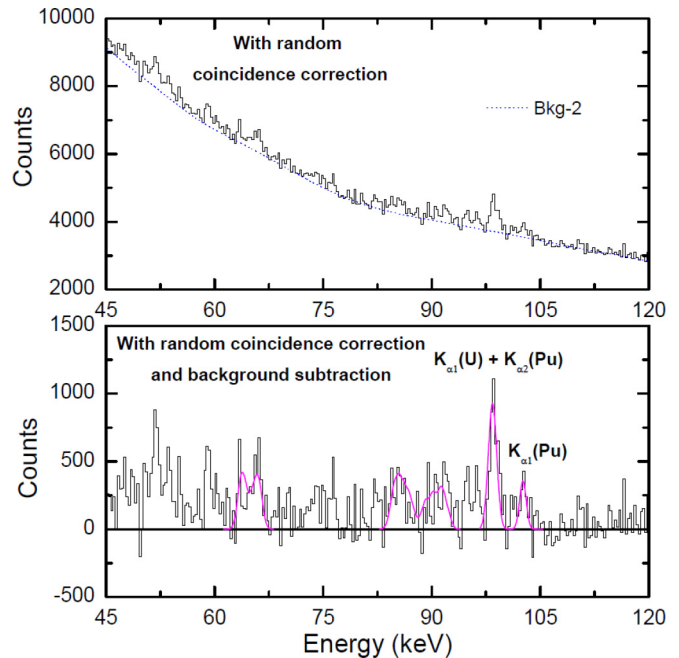


FIG. 10. Random corrected coincidence photon spectrum with Bkg-2 (dotted blue) background is shown in the upper panel. Bkg-2 subtracted coincidence spectrum is shown in the lower panel. GEANT3 simulation of a fission fragment  $K$  x ray at 65 keV and a fission fragment  $\gamma$  ray at 88 keV are shown in magenta color. The peaks around 98.4 and 103 keV are also shown in magenta color.

## 2. Analysis with Bkg-2

We have repeated the analysis using the slightly lower Bkg-2 (dotted blue background) of Fig. 4. We show Bkg-2 drawn on the random corrected coincidence spectrum in Fig. 10 (upper panel) and the corresponding spectrum after subtracting out the background in Fig. 10 (lower panel) where the peaks at 103 and 98.4 keV and broad double-humped peaks at 65 keV ( $K_{\alpha 1}$  x ray from iridium) and 88 keV (fission fragment  $\gamma$  ray) have been shown by magenta color curves. Considering the suppression factor of the uranium atomic excitation lines in the true coincidence spectrum compared to their yields in the singles spectrum, we estimate that more than half of the peak area seen around 103 keV in the random corrected true coincidence spectrum (Fig. 10) should be the  $K$  x-ray photons in true coincidence with the fission fragments.

In Fig. 11, we show the random and background subtracted true coincidence spectrum from 96.6 to 107 keV. In order to determine whether the peak around 103 keV is due to fission fragment  $\gamma$ -ray or a plutonium  $K$  x-ray line, we have performed a similar analysis as discussed earlier for Bkg-1. The data points were first fitted by GEANT3 simulation [23] of a sharp fission fragment  $\gamma$  ray and then an additional area at 98.4 keV was added to obtain the best fit ( $\chi^2 = 1.55$ ) shown by a dashed blue curve. This additional added Gaussian peak area at 98.4 keV should be the remnant of the uranium  $K_{\alpha 1}$  line and the ratio of relative efficiency corrected remnants of uranium  $K_{\alpha 2}$  (94.65 keV) to uranium  $K_{\alpha 1}$  (98.4 keV) becomes  $1.37 \pm 0.25$ , in disagreement with the known branching ratio of 0.625 [29]. It is possible to improve the overall fit in the 96.6- to 105.3-keV

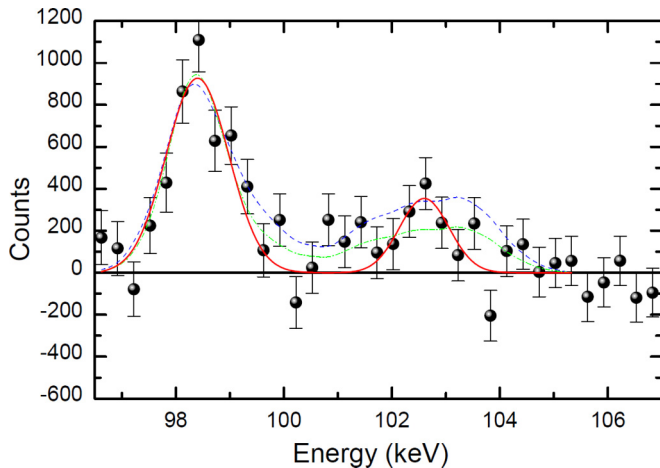


FIG. 11. Bkg-2 subtracted coincidence photon spectrum with the statistical error bars is shown in the energy range from 96.6 to 107 keV. Dashed blue and dot-dashed green curves represent GEANT3 simulation of a sharp 101-keV  $\gamma$ -ray line from a fission fragment with additional yield at 98.4 keV. The solid red curve shows Gaussian fit of the data points with two isolated peaks (see text for details).

region by adjusting the areas under the added uranium  $K_{\alpha 1}$  line and GEANT3 simulated spectrum simultaneously and the best fit shown by the dot-dashed green curve gives a reduced  $\chi^2 = 1.1$  as shown in Fig. 11. However the corresponding ratio of the relative efficiency corrected remnants of uranium  $K_{\alpha 2}$  to uranium  $K_{\alpha 1}$  yields remains  $0.95 \pm 0.17$ , in disagreement with the known branching ratio of 0.625 [29]. The spectrum has also been analyzed assuming the peak around 103 keV as the plutonium  $K_{\alpha 1}$  line and its associated  $K_{\alpha 2}$  line overlaps with the 98.4-keV uranium  $K_{\alpha 1}$  line. In Fig. 11, the solid red curve is the best fit with two isolated Gaussian peaks and the peak positions are at 98.4 and 102.6 keV (FWHM = 1 keV). The best fit gives a reduced  $\chi^2 = 1.1$ . The estimated plutonium  $K_{\alpha 2}$  yield (based on the yield at 103 keV after correcting for random coincidences) has been subtracted out from the fitted Gaussian peak area at 98.4 keV to obtain the yield of the remnant uranium  $K_{\alpha 1}$  line. The ratio of the remnants of uranium  $K_{\alpha 2}$  to uranium  $K_{\alpha 1}$  yield (after relative efficiency correction) is  $0.64 \pm 0.15$ , in good agreement with the known branching ratio of 0.625 [29]. Hence, although both the dot-dashed green curve and the solid red curve fit the data points equally well and both of them are statistically significant, the interpretation in terms of a fission fragment  $\gamma$  ray cannot reproduce the expected ratio of the remnants of uranium  $K_{\alpha 2}$  to uranium  $K_{\alpha 1}$  lines, whereas the interpretation in terms of the plutonium  $K_{\alpha 1}$  line around 103 keV reproduces the ratio of the remnants of uranium  $K_{\alpha 2}$  to uranium  $K_{\alpha 1}$  lines very well. Moreover, unlike the spectral shape around 103 keV, the humps around 88 keV could only be fitted well by GEANT3 simulation of a fission fragment  $\gamma$  ray, thus demonstrating a qualitatively different spectral shape around 103 keV.

In Fig. 12, we show the photon spectrum in the energy range from 100.5 to 105.9 keV in coincidence with the fission fragments. The dot-dashed green curve is the best fit (reduced  $\chi^2 = 1.2$ ) with GEANT3 simulation of the high energy hump of

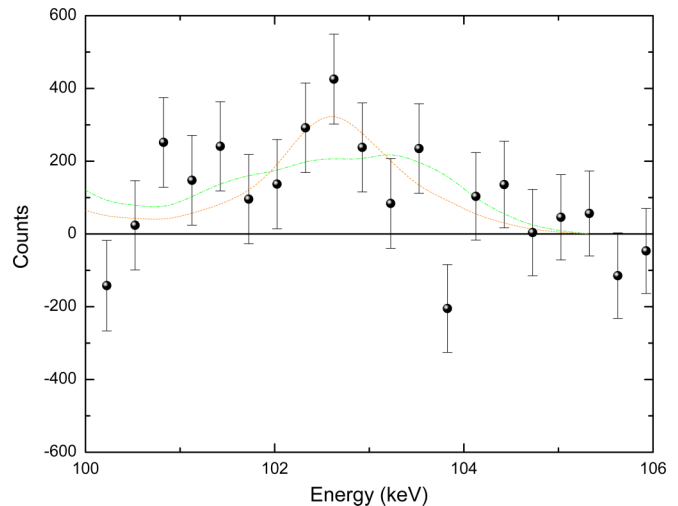


FIG. 12. Random corrected coincidence spectrum for Bkg-2 subtraction with statistical error bars in the energy range from 100.5 to 105.9 keV. Dot-dashed green curve is the high energy hump for best fitted GEANT3 simulation of 101-keV fission fragment  $\gamma$  ray. Dotted red curve is the best fit for a combination of GEANT3 simulation of fission fragment  $\gamma$ -ray and a Gaussian peak around 103 keV with FWHM = 1 keV as discussed in the text.

a fission fragment  $\gamma$  ray. Now let us add a narrow (FWHM = 1 keV) Gaussian peak centered around 103 keV with the GEANT3 simulation of the fission fragment  $\gamma$  ray, assuming that both the broad hump of the fission fragment  $\gamma$  ray and a narrow Gaussian peak could be present. The areas under the broad hump and the Gaussian peak have been adjusted to obtain the best fit of the data points. We not only obtain a very good fit (reduced  $\chi^2 = 1.0$ ), but more importantly, the best fit as shown by the dotted red line significantly reduces the contribution of the broad hump and projects out the Gaussian peak, indicating that the Gaussian peak is a better description of the data points. However, unlike in Fig. 8, the Gaussian peak in Fig. 12 is clearly riding on a background, indicating that the background curve (Bkg-2) on the coincidence spectrum (Figs. 4 and 10) has been drawn somewhat below the optimum background level. From Fig. 12, we obtain that the FWHM of the Gaussian peak around 103 keV is  $(1 \pm 0.3)$  keV, in good agreement with that obtained from Fig. 7. Using the procedure described earlier and taking the area of 103 keV Gaussian peak from Fig. 12, we have obtained plutonium  $K$  x-ray multiplicity per fission event ( $\sigma_K/\sigma_f$ ) with a statistical uncertainty of  $\approx 30\%$ . Taking  $P_K = 7.2 \times 10^{-4}$  (as obtained earlier), we get the percentage of slow fission events (corresponding to an extreme bimodal fission time distribution)  $\frac{\sigma_K}{P_K \sigma_f} = 0.83$ . The percentage of slow fission events would increase for any other fission time distribution. Even after considering the uncertainty on  $P_K$  as discussed in a previous section, we have a strong ground to conclude qualitatively that most of the fission events are slow for a realistic fission time distribution.

In this case also, the candidate peak is at 102.8 keV, just below the characteristic plutonium  $K_{\alpha 1}$  line (103.7 keV) and no narrow peak is seen at 103.7 keV. Assuming that 102.8-keV peak is a part of a broad fission fragment  $\gamma$ -ray peak or an

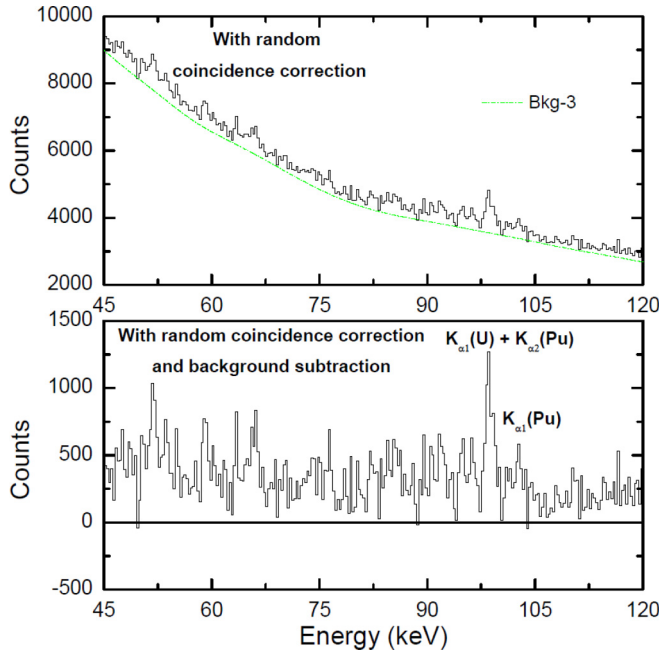


FIG. 13. Random corrected coincidence photon spectrum with Bkg-3 (dashed green) background is shown in the upper panel. Bkg-3 subtracted coincidence photon spectrum is shown in the lower panel.

unknown narrow peak, we have attempted to extract the area of a narrow peak ( $\text{FWHM} = 1 \text{ keV}$ ) at  $103.7 \text{ keV}$  and find that the peak area comes out negative, consistent with zero within the error bars. So, for a no shift scenario, our observations would contradict earlier claims of significant percentage [1,3] of slow fission events as obtained by the atomic techniques for similarly excited uraniumlike nuclei. Hence, the results obtained by using Bkg-1 and Bkg-2 are qualitatively similar.

### 3. Analysis with Bkg-3

As shown in Fig. 4, Bkg-3 (dot-dashed green background curve) has been drawn significantly below Bkg-2. Let us first discuss whether the results obtained by drawing Bkg-3 look reasonable and self-consistent. In Fig. 13, upper panel, we show Bkg-3 drawn on the random corrected coincidence spectrum and in Fig. 13, lower panel, we show the corresponding spectrum after the subtraction of Bkg-3. There is hardly any negative count in the background subtracted spectrum implying that the background was drawn too low. In Fig. 14, we show the Bkg-3 subtracted spectrum in the region from  $96.6$  to  $107 \text{ keV}$ . In this case, a Gaussian fit of the data points around  $103 \text{ keV}$  gives a broad peak with the peak position at  $102.6 \text{ keV}$  and  $\text{FWHM} = 4.4 \text{ keV}$  as shown by the red curve in Fig. 14. The fit gives a reduced  $\chi^2 = 1.4$  and a large Gaussian area. The extrapolation of the Gaussian fit is shown by the dotted red curve. However, a linear fit (shown by the dot-dashed green line in Fig. 14) gives a better fit ( $\chi^2 = 1.26$ ) for those data points indicating that if there is a peak, it is riding on a high background. If this peak around  $103 \text{ keV}$  is interpreted as the plutonium  $K_{\alpha 1}$  x-ray line, then on one hand, its large width would imply a short fission time and on the other hand its large  $K$  x-ray yield would imply a long fission time. The

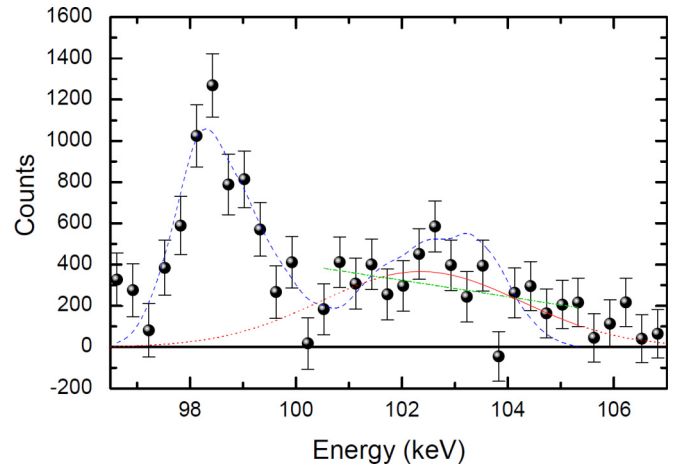


FIG. 14. Random corrected coincidence spectrum for Bkg-3 subtraction with the statistical error bars is shown in the energy range from  $96.6$  and  $107 \text{ keV}$ . Dash blue curve represents GEANT3 simulation of a sharp  $101\text{-keV}$   $\gamma$ -ray line from a fission fragment with additional yield at  $98.4 \text{ keV}$ . The red curve and dot-dashed green line show the Gaussian and linear fits of the data points around  $103 \text{ keV}$  respectively. Solid red curve indicates the region used for Gaussian fit and the dotted red curve is the extrapolation of the Gaussian fit (see text for details).

combination of a large width and large yield could be made consistent only for an unrealistically high value (of the order of 1) of  $P_K$  (probability of creation of  $K$  vacancy in plutonium). In Fig. 14, the dashed blue curve is the best (reduced  $\chi^2 = 1.6$ ) GEANT3 simulation [23] of a fission fragment  $\gamma$  ray with an added additional area at  $98.4 \text{ keV}$  due to imperfect cancellation of the random coincidence events. The additional area should be the remnant of a uranium  $K_{\alpha 1}$  ( $98.4 \text{ keV}$ ) line and the ratio of relative efficiency corrected remnants of the uranium  $K_{\alpha 2}$  ( $94.65 \text{ keV}$ ) to  $K_{\alpha 1}$  ( $98.4 \text{ keV}$ ) line is  $1.8 \pm 0.4$ , in disagreement with the known branching ratio of  $0.625$  [28] by more than two standard deviations. If we only fit the data points around  $103 \text{ keV}$  (from  $100.8$  to  $105.3 \text{ keV}$ ) by the broad high energy hump of fission fragment  $\gamma$  ray as obtained from GEANT3 simulation, then the best fit gives a reduced  $\chi^2 = 2$ , implying a rather poor fit. Hence, it is clear that Bkg-3 of Fig. 4 is too low to be considered as a plausible background.

## IV. CONCLUSION

We have studied the spectrum of photons emitted in coincidence with the fission fragments produced in the fusion reaction  ${}^4\text{He} + {}^{238}\text{U}$  at  $E_{\text{LAB}}({}^4\text{He}) = 60 \text{ MeV}$  with a high energy resolution of  $1 \text{ keV}$ . This experiment has higher sensitivity than previous experiments using heavy ion reactions, allowing us to see individual  $K$  x-ray peaks (from plutonium) above background. We have found a narrow peak of intrinsic  $\text{FWHM} \leq 0.6 \text{ keV}$  at  $(102.8 \pm 0.5) \text{ keV}$ , just below the expected plutonium  $K_{\alpha 1}$  position of  $103.7 \text{ keV}$ . On the basis of spectral shape and other characteristics, we have concluded that this peak can be attributed to the plutonium  $K_{\alpha 1}$  line. From the intrinsic width of the plutonium  $K$  x-ray peaks, it follows that the fission time of slow fission events is  $> 1 \times 10^{-18} \text{ s}$  using quantum energy-time uncertainty principle without requiring knowledge of any other

parameters. The minimum percentage of slow fission events was determined from the  $K$  x-ray multiplicity per fission in the same way as other experiments [5,6], taking  $P_K \geq 7.2 \times 10^{-4}$ . Combining  $K$  x-ray multiplicity results with the fission time of slow fission events as obtained from the width of plutonium  $K$  x-ray lines, we have a strong ground to conclude that most of the fission events are slow for a realistic fission time distribution, in agreement with the previous results obtained using atomic techniques [1,3].

We have performed atomic physics calculations indicating that a shift of plutonium  $K$  x-ray lines from the standard positions by  $(0.9 \pm 0.5)$  keV is plausible, if the rotating fissioning plutonium nucleus would spend most of its long fission time with highly deformed dumbbell-type shapes. A combined dynamical and statistical model [39] and prefission neutron multiplicity results [20] support the idea that the fissioning nucleus spends most of its time during saddle to scission transitions in highly deformed dumbbell-type shapes [11]. On the other hand, long mean fission time ( $\tau_f > 10^{-18}$  s) could be obtained [13] in the framework of Langevin fluctuation-dissipation dynamical calculations [12,13] by increasing friction inside the saddle. The vastly different results obtained by nuclear and atomic techniques have not yet been properly reconciled [14].

Alternatively, if the observed narrow peak at 102.8 keV is not the plutonium  $K_{\alpha 1}$  line, then the absence of a peak at 103.7 keV would contradict earlier claims [1,3] of significant (>70% or about 100%) percentage of slow fission events

obtained by atomic techniques and the results would be in agreement with prefission neutron multiplicity results [10] and expectations from simple statistical models.

In summary, we find a small shift of plutonium  $K$  x-ray lines that could not be observed in earlier lower resolution experiments and find that most of the fission events are slow, in agreement with the earlier results [1,3]. However, the shift implies that the fissioning nucleus spends most of its long fission time in highly deformed dumbbell-type shapes. Alternatively, if this requirement to explain the shift is not considered plausible, the absence of a peak at the expected position would contradict earlier atomic technique results.

#### ACKNOWLEDGMENTS

We thank P. Indelicato (CNRS, Laboratoire Kastler Brossel, France) and A. N. Artemyev (University of Kassel, Kassel, Germany) for carrying out atomic calculations and many useful discussions. We acknowledge many useful discussions with J. Sadhukhan, Amit Roy (Variable Energy Cyclotron Center, Kolkata, India) and R. Vandenbosch (University of Washington, Seattle, USA). We thank M. Saha Sarkar (Saha Institute of Nuclear Physics, Kolkata, India) and T. Christophe (IRFU, CEA, Université Paris-Saclay, France) for providing us with LEPS detectors and photovoltaic cells respectively. A. Ray acknowledges financial assistance from Science and Engineering Research Board (Government of India) Grant No. EMR/2016/001914.

- 
- [1] J. D. Molitoris, W. E. Meyerhof, C. Stoller, R. Anholt, D. W. Spooner, L. G. Moretto, L. G. Sobotka, R. J. McDonald, G. J. Wozniak, M. A. McMahan, L. Blumenfeld, N. Colonna, M. Nessi, and E. Morenzoni, *Phys. Rev. Lett.* **70**, 537 (1993).
  - [2] F. Goldenbaum, M. Morjean, J. Galin, E. Liénard, B. Lott, Y. Périer, M. Chevallier, D. Dauvergne, R. Kirsch, J. C. Poizat, J. Remillieux, C. Cohen, A. L'Hoir, G. Prévot, D. Schmaus, J. Dural, M. Toulemonde, and D. Jacquet, *Phys. Rev. Lett.* **82**, 5012 (1999).
  - [3] J. U. Andersen, J. Chevallier, J. S. Forster, S. A. Karamian, C. R. Vane, J. R. Beene, A. Galindo-Uribarri, J. G. del Campo, C. J. Gross, H. F. Krause, E. Padilla-Rodal, D. Radford, D. Shapira, C. Broude, F. Malaguti, and A. Uguzzoni, *Phys. Rev. C* **78**, 064609 (2008).
  - [4] M. Morjean, D. Jacquet, J. L. Charvet, A. L'Hoir, M. Laget, M. Parlog, A. Chbihi, M. Chevallier, C. Cohen, D. Dauvergne, R. Dayras, A. Drouart, C. Escano-Rodriguez, J. D. Frankland, R. Kirsch, P. Loutesse, L. Nalpas, C. Ray, C. Schmitt, C. Stodel *et al.*, *Phys. Rev. Lett.* **101**, 072701 (2008).
  - [5] H. W. Wilschut and V. L. Kravchuk, *Nucl. Phys. A* **734**, 156 (2004).
  - [6] M. O. Frégeau, D. Jacquet, M. Morjean, E. Bonnet, A. Chbihi, J. D. Frankland, M. F. Rivet, L. Tassan-Got, F. Dechery, A. Drouart, L. Nalpas, X. Ledoux, M. Parlog, C. Ciortea, D. Dumitriu, D. Fluerasu, M. Gugiu, F. Gramegna, V. L. Kravchuk, T. Marchi, D. Fabris, A. Corsi, and S. Barlini, *Phys. Rev. Lett.* **108**, 122701 (2012).
  - [7] J. Töke, R. Bock, G. X. Dai, A. Gobbi, S. Gralla, K. D. Hildenbrand, J. Kuzminski, W. F. J. Müller, A. Olmi, H. Stelzer, B. B. Back, and S. Bjørnholm, *Nucl. Phys. A* **440**, 327 (1985).
  - [8] R. du Rietz, D. J. Hinde, M. Dasgupta, R. G. Thomas, L. R. Gasques, M. Evers, N. Lobanov, and A. Wakhle, *Phys. Rev. Lett.* **106**, 052701 (2011).
  - [9] D. J. Hinde, D. Hilscher, H. Rossner, B. Gebauer, M. Lehmann, and M. Wilpert, *Phys. Rev. C* **45**, 1229 (1992).
  - [10] A. Saxena, A. Chatterjee, R. K. Choudhury, S. S. Kapoor, and D. M. Nadkarni, *Phys. Rev. C* **49**, 932 (1994).
  - [11] A. Bulgac, P. Magierski, K. J. Roche, and I. Stetcu, *Phys. Rev. Lett.* **116**, 122504 (2016).
  - [12] I. Gontchar, M. Morjean, and S. Basnary, *Europhys. Lett.* **57**, 355 (2002).
  - [13] D. Jacquet and M. Morjean, *Prog. Part. And Nucl. Phys.* **63**, 155 (2009).
  - [14] A. K. Sikdar, A. Ray, and A. Chatterjee, *Phys. Rev. C* **93**, 041604 (2016).
  - [15] R. Anholt, *Rev. Mod. Phys.* **57**, 995 (1985).
  - [16] J. F. Chemin *et al.*, *Nucl. Phys. A* **331**, 407 (1979).
  - [17] S. Röhl, S. Hoppenau, and M. Dost, *Nucl. Phys. A* **369**, 301 (1981).
  - [18] J. F. Chemin *et al.*, *Z. Phys. D* **2**, 161 (1986).
  - [19] F. Azaiez, M. M. Aleonard, S. Andriamonje, J. F. Chemin, J. N. Scheurer, D. W. Spooner, J. P. Thibaud, J. F. Bruandet, E. Liatard, F. Beck, and G. Costa, *Phys. Rev. Lett.* **65**, 305 (1990).
  - [20] J. P. Lestone, *Phys. Rev. Lett.* **70**, 2245 (1993).

- [21] F. Puhlhofer, *Nucl. Phys. A* **280**, 267 (1977).
- [22] N. N. Ajitanand, R. P. Anand, S. R. S. Murthy, and K. N. Iyengar, *Nucl. Instrum. Methods Phys. Res. A* **300**, 354 (1991).
- [23] R. Brun *et al.*, GEANT3, CERN/DD/EE/84-1, 1986.
- [24] G. Deconninck and N. Longequeue, *Phys. Rev. Lett.* **30**, 863 (1973).
- [25] I. Ahmad, J. Hines, and J. E. Gindler, *Phys. Rev. C* **27**, 2239 (1983).
- [26] D. Ward *et al.*, *Nucl. Phys. A* **600**, 88 (1996).
- [27] N. R. Johnson *et al.*, *Phys. Rev. C* **12**, 1927 (1975).
- [28] G. Lapicki, *J. Phys. Chem. Ref. Data* **18**, 111 (1989).
- [29] C. M. Lederer and V. S. Shirley, *Table of Isotopes* (John Wiley & Sons, Inc., New York, 1978).
- [30] V. E. Viola, K. Kwiatkowski, and M. Walker, *Phys. Rev. C* **31**, 1550 (1985).
- [31] R. K. Jain, S. K. Bose, and J. Rama Rao, *Pramana - J. Phys.* **45**, 519 (1995).
- [32] M. O. Krause and J. H. Oliver, *J. Phys. Chem. Ref. Data* **8**, 329 (1979).
- [33] V. L. Kravchuk, A. M. van den Berg, F. Fleurot, M. A. de Huu, H. Löhner, H. W. Wilschut, M. Polasik, M. Lewandowska-Robak, and K. Slabkowska, *Phys. Rev. A* **64**, 062710 (2001).
- [34] V. L. Kravchuk, H. W. Wilschut, A. M. van den Berg, B. Davids, F. Fleurot, M. Hunyadi, M. A. de Huu, H. Löhner, and A. van der Woude, *Phys. Rev. A* **67**, 052709 (2003).
- [35] T. A. Carlson, C. W. Nestor, Jr., T. C. Tucker, and F. B. Malik, *Phys. Rev.* **169**, 27 (1968).
- [36] P. Sharma and T. Nandi, *Phys. Rev. Lett.* **119**, 203401 (2017).
- [37] P. Indelicato (private communication).
- [38] Y. S. Kozhedub, O. V. Andreev, V. M. Shabaev, I. I. Tupitsyn, C. Brandau, C. Kozhuharov, G. Plunien, and T. Stöhlker, *Phys. Rev. A* **77**, 032501 (2008).
- [39] P. Fröbrich and I. I. Gontchar, *Phys. Rep.* **292**, 131 (1998).
- [40] A. N. Artemyev (private communication).